UNIVERSITÀ DEGLI STUDI DI BRESCIA

Dipartimento di Medicina Molecolare e Traslazionale

UNIVERSITÀ
DEGLI STUDI
DI BRESCIA

DOTTORATO DI RICERCA IN

Genetica Molecolare, Biotecnologie e Medicina Sperimentale

settore scientifico disciplinare

BIO/13

CICLO

XXXV

TITOLO TESI

RNA editing of CYFIP2 regulates actin related cellular migration and neuronal development *in vitro*

RELATORE: Prof. Alessandro Barbon

DOTTORANDO: Luca La Via

Anno Accademico 2021/2022

INDEX

LIST OF ABBREVIATIONS

Abbreviation	Definition
ABI2	Arg-Binding Protein Interactor 2
ADAR	Adenosine Deaminase Acting on RNA
AGO2	Argonaute RISC Catalytic Component 2
APP	Amyloid Precursor Protein
ARC	Activity-regulated cytoskeleton-associated protein
Arp 2/3	Actin Related Protein 2/3
ASD	Autism spectrum disorder
BLCAP	Bladder Cancer Associated Protein
C57BL/6	C57 black 6 mouse
CaMKII	Ca2+/calmodulin-dependent protein kinase II
Cas9	CRISPR associated protein 9
CD4+	CD4 T lymphocytes
CDS	Coding Sequence
CNS	Central Nervous System
CRISPR	Clustered Regularly Interspaced Short Palindromic Repeats
cryo-EM	cryo-electron microscopy
CYFIP1	Cytoplasmic FMRP Interacting Protein 1
CYFIP2	Cytoplasmic FMRP Interacting Protein 2
DIV	Day *In Vitro*
DSB	Double Strand Break
E2F1	E2F Transcription Factor 1
ECS	Editing Complementary Sequence

eIF4E	Eukaryotic translation initiation factor 4E
FLNA	Filamin A
FMRP	Fragile X Messenger Ribonucleoprotein
FXR1P	Fragile X related protein 1
FXR1P	Fragile X related protein 2
FXS	Fragile X syndrome
GTPase	GTP-binding proteins
HSPC300	Haematopoietic Stem/Progenitor Cell Protein 300
ID	Intellectual disability
IGFBP7	Insulin Like Growth Factor Binding Protein 7
KD	Gene *Knock-Down*
kDa	Kilo Dalton
KI	*Gene Knock-In*
KO	*Gene Knock-Out*
MAP1B	Microtubule Associated Protein 1B
miRNA	Micro RNA
MOI	Multiplicity Of Infection
mTOR	Mechanistic Target Of Rapamycin Kinase
NCKAP1	NCK Associated Protein 1
NPFs	Nucleation-promoting factors
Nt	Nucleotide
P53	Tumor protein P53
PFA	Paraformaldehyde
PDB	Protein Data Bank
PIR121	P53-Inducible Protein 121
PUM1	Pumilio1
RAC1	Ras-related C3 botulinum toxin substrate 1

RGCs	Retinal glial cells
RHO	Ras Homologous protein family
RT	Room Temperature
S6K1	Ribosomal protein S6 kinase beta-1
SCAR	Suppressor of cAMP Receptor
scRNAseq	Single-cell RNA sequencing
sgRNA	Single Guide RNA
SRA-1	Steroid Receptor RNA Activator 1
UTRs	UnTranslated Region
WASP	Wiskott–Aldrich syndrome protein
WAVE	WASP family Verprolin homolog
WCA	WH2-central-acidic motif
WH2 domain	WASP-Homology 2 domain
WRC	Wave Regulatory Complex
WT	Wild Type

ABSTRACT

Cytoplasmic FMRP Interacting Protein 2 (CYFIP2) è una proteina originariamente identificata come componente del Wave Regulatory Complex (WRC) e come interattore di Fragile-X Messenger Ribonucleoprotein (FMRP). È interessante notare che il trascritto di *CYFIP2* è sottoposto alla reazione di editing dell'RNA, un meccanismo epi-trascrittomico catalizzato dagli enzimi ADAR, che porta l'Adenosina (A) alla deaminazione a Inosina (I). In seguito al processo di traduzione, l'editing di *CYFIP2* comporta una sostituzione K/E dell'amminoacido in posizione 320 sia in proteine umane che di topo. Il suo significato funzionale è ancora sconosciuto. Questo studio vuole indagare le potenziali implicazioni di questo processo nei fenomeni correlati alla dinamica dell'actina durante la migrazione cellulare, lo sviluppo degli assoni e la sinaptogenesi nelle cellule neuronali.

I nostri risultati mostrano che l'editing dell'RNA di *CYFIP2* aumenta durante lo sviluppo neurale. È un processo attivo solo nel sistema nervoso centrale ed è specificatamente regolato in diverse aree cerebrali. Tale processo può inoltre essere modulato dall'attività neuronale. Questi dati, nel loro insieme, indicano come una corretta regolazione dell'editing di *CYFIP2* sia importante durante lo sviluppo e la funzione neuronale. La sua disregolazione potrebbe essere quindi coinvolta in disturbi dello sviluppo neurologico.

Per ottenere maggiori informazioni sul ruolo dell'editing dell'RNA di *CYFIP2*, abbiamo inizialmente deleto il gene *CYFIP2* attraverso la tecnica di CRISPR-Cas9 in cellule di neuroblastoma SHSY-5Y, e abbiamo sovraespresso le varianti di CYFIP2 non editate ed editate (rispettivamente, HA-CYFIP2-320K e HA-CYFIP2-320E) nelle linee *KO*, attraverso trasduzione lentivirale. La sovra espressione di entrambe le varianti è in grado di ripristinare il fenotipo morfologico delle cellule analizzate. I nostri risultati mostrano differenze funzionali delle proteine CYFIP2 editate e non editate nella regolazione della migrazione cellulare. In particolare, la variante editata (CYFIP2-E) presenta una maggiore capacità di migrare, sia in condizioni di deprivazione di siero che sotto stimolazione di fattori di crescita. Questi dati indicano che la reazione di editing potrebbe essere coinvolta nella dinamica di migrazione cellulare.

Poiché la proteina CYFIP2 è espressa principalmente nei neuroni e la reazione di editing dell'RNA è attiva solo nel sistema nervoso centrale, abbiamo investigato il ruolo delle varianti di CYFIP2

durante lo sviluppo neuronale. A tale scopo, abbiamo utilizzato un consolidato modello di differenziamento neuronale in cellule SH-SY5Y, basato sull'applicazione di acido retinoico (RA) e il fattore di crescita neuronale BDNF per monitorare la conversione di cellule indifferenziate in cellule con morfologia simil-neuronale altamente polarizzate.

I nostri risultati dimostrano chiaramente che le cellule *KO* per il gene *CYFIP2* hanno perso la capacità di produrre una caratteristica morfologia simil-neuronale dopo il differenziamento, mentre la sovra espressione delle varianti di editing ne ripristina la capacità differenziativa. Tuttavia, non è stato possibile rilevare differenze tra le popolazioni di cellule K ed E, indicando come la proteina CYFIP2 sia importante per il differenziamento neuronale, ma il processo di editing potrebbe non avere un ruolo in questo processo.

Per approfondire il ruolo delle varianti K ed E in un sistema maggiormente fisiologico, abbiamo deciso di utilizzare colture neuronali primarie di roditore. L'espressione di CYFIP2 endogena è stata silenziata utilizzando specifici shRNA e le colture cellulari sono state trasdotte con vettori lentivirali esprimenti le varianti K o E di CYFIP2. Durante la maturazione neuronale sono stati analizzati parametri morfologici relativi allo sviluppo assonale delle cellule neuronali. Abbiamo riscontrato una differenza statisticamente significativa tra i neuroni che esprimono le varianti non editate ed editate nel numero di ramificazioni, nella lunghezza totale e nell'indice di complessità degli assoni analizzati.

Abbiamo inoltre applicato il nostro modello basato sulle colture primarie ippocampali per cercare di capire se l'editing di *CYFIP2* possa essere implicato nel processo di sinaptogenesi. I nostri risultati mostrano come la frequenza delle spine venga drasticamente ridotta nelle cellule in cui la proteina CYFIP2 è stata silenziata. La popolazione di cellule che esprimono in maggioranza la variante di CYFIP2 non editata (K) non portano ad un ripristino nella frequenza nelle spine che,al contrario si osserva nelle cellule che si sviluppano esprimendo la variante editata di CYFIP2 (E).

Nel loro insieme questi risultati mostrano un chiaro ruolo della proteina CYFIP2 nella regolazione dello sviluppo assonale durante le prime fasi dello sviluppo in vitro e durante il processo di sinaptogenesi. La reazione K/E di editing dell'RNA del trascritto risulta inoltre importante in entrambi i processi studiati.

1 INTRODUCTION

1.1 Regulations of actin polymerisation

A variety of eukaryotic cell functions, including cell migration and vesicle trafficking, are driven by the dynamic rearrangement of the actin cytoskeleton. At the molecular level, actin is a globular protein of ~375 residues. Under physiological salt levels actin monomers (G-actin) spontaneously polymerize to filamentous actin (F-actin), although ATP-actin monomers are primarily responsible for this process (Pollard, 2016). Actin filament nucleation in cells is strictly controlled by specific regulatory proteins known as "nucleators." These proteins influence actin network architecture in addition to promoting the growth of new filaments. The two stereotypical actin filament structures are branched filament networks formed by the Arp2/3 complex, and long linear filaments formed by Formins and Ena/VASP (Lappalainen et al., 2022). The Arp2/3 complex is a heptameric complex composed of two actin-related proteins (ARP2 and ARP3) and five scaffolding subunits (ARPC1 to ARPC5). Arp2/3 activation is mediated by so-called nucleation-promoting factors (NPFs) (Machesky et al., 1999) (Fig. 1). The Wiskott–Aldrich syndrome protein (WASP) family proteins and the WAVE family protein complexes are the most important for endocytosis and cell migration, respectively.

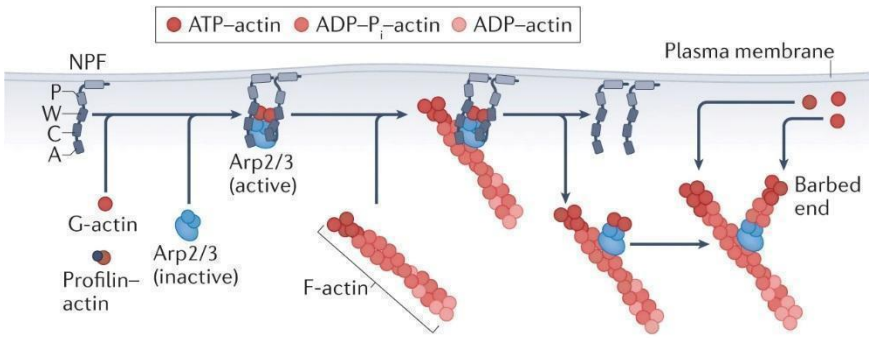

Figure 1

Formation of branched actin networks. Membrane-anchored nucleation-promoting factors (NPFs) harbour four characteristic domains at their carboxy terminus: the polyproline (P), WH2 (W), central (C) and acidic (A) domains. Two NPFs recruit and activate an Arp2/3 complex by binding actin monomers with their W domains, while binding Arp2 and Arp3 subunits with their C and A domains. Activated Arp2/3 can bind to the side of an actin filament to induce the growth of a branched daughter filament, once the NPFs have detached from the Arp2/3. Modify from (Lappalainen et al., 2022).

Dysregulation of this structure is strongly linked to a number of pathologies, including cancer, immunological deficiencies, and neurological disorders.

Moreover, actin dynamics are fundamental for determining the shape and function of cells. In neurons, one of the most remarkable examples of cellular polarisation, the coordination of actin filaments dynamics is crucial to the development, maturation, and function of cells. Additionally, the remodelling of the underlying actin cytoskeleton is a large determinant in how dendritic spine size and shape vary in relation to excitatory synapses functions. Spine development, plasticity and synaptic function all depend on actin dynamics (Fig. 2, bottom). This process is one of the bases underlying synaptic plasticity processes (Citri & Malenka, 2008).

In addition to synaptic impacts, regulation of actin cytoskeleton dynamics modifies and guides the extension of axonal projections from neurons to their specific destination for synaptic connections (Fig. 2, top), processes essential for the development of brain circuit complexity (Shah & Rossie, 2018).

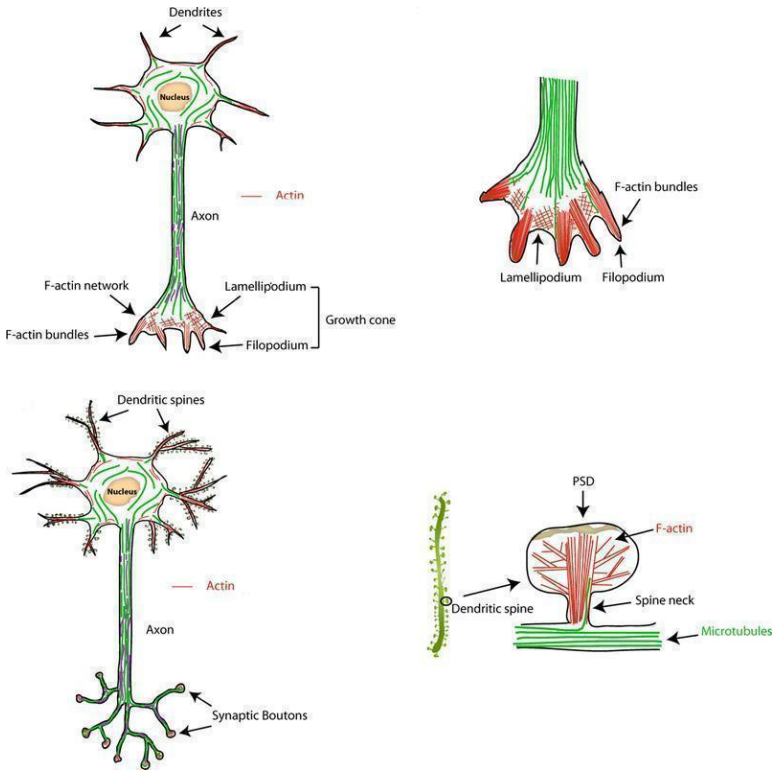

Figure 2

Actin cytoskeletal network in growth cones and dendritic spines. Components of the neuronal cytoskeleton in a developing neuron. The neuronal cytoskeleton comprises actin filaments (red), microtubules (green), and neurofilaments (purple). The axonal growth cone is composed of lamellipodia and filopodia, both of which are highly enriched in actin filaments. Lamellipodia consist of a dense F-actin network, and filopodia contain bundled F-actin (Top). A mature neuron showing dendritic spines and synaptic boutons. Dendritic spines are highly dynamic membranous protrusions on postsynaptic dendrites, which have a rich F-actin cytoskeleton (bottom). Modify from (Shah & Rossie, 2018).

1.1.1 WASP family members

In a variety of functions, including cell migration and intracellular vesicle trafficking, the Wiskott-Aldrich Syndrome Protein (WASP) family members are essential for driving Arp2/3 complex-mediated actin assembly (Campellone & Welch, 2010) (Fig. 3).

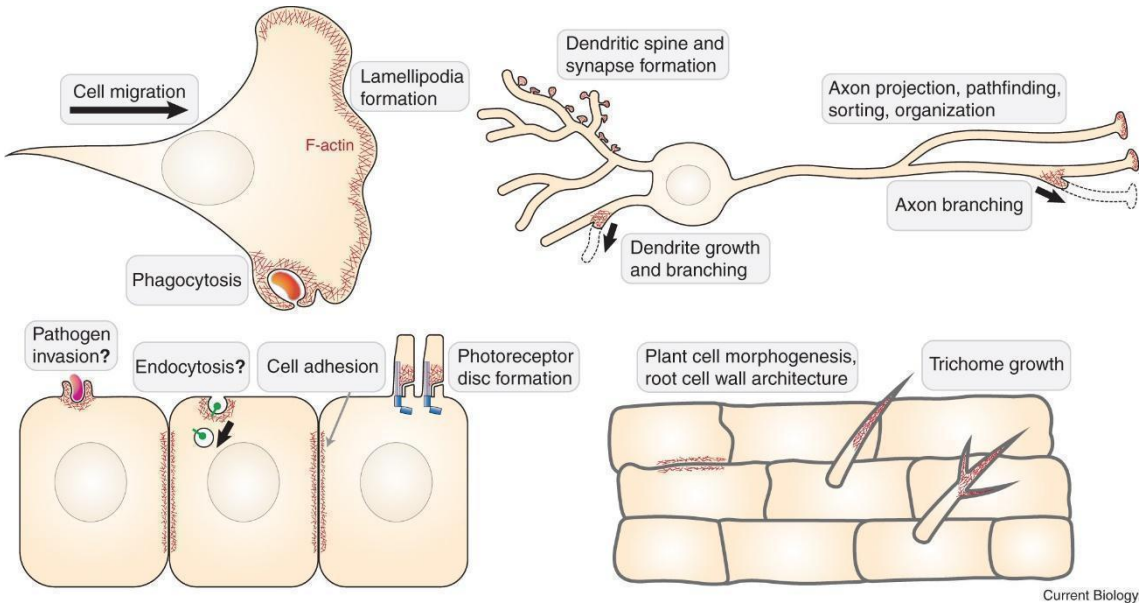

Figure 3

Model of the major cellular activities that Wasp Family members-mediated actin network assembly controls. From (Rottner et al., 2021).

These proteins have a common WCA (WH2-central-acidic) motif at their C-terminus that can bind to and activate the Arp2/3 complex, resulting in the formation of branching actin networks at membranes (Alekhina et al., 2017). At the basal state, the majority of WASP-family proteins are inhibited. Blocking is achieved by keeping their WCA domain confined, either in trans within large multi-protein complexes like WAVE and WASH3 (Padrick et al., 2008), or in cis within a single polypeptide chain, as in WASP and N-WASP.

WAVE (WASP family Verprolin homolog; also known as SCAR for Suppressor of cAMP Receptor) is one of the WASP-family proteins that is specifically controlled by constitutive incorporation into the ~400 kDa WAVE Regulatory Complex (WRC).

1.1.2 Wave Regulatory Complex (WRC)

The WRC has received much interest from biologists and biochemists who are trying to unravel its structure, regulation, and function since the Kirschner lab first discovered it in 2002 through biochemical purification (Gautreau et al., 2004). This is due to the WRC's role in membrane protrusion, cell motility, and numerous clinical diseases, as well as the fact that its size and intricacy make it an intriguing model for studying membrane-to-actin signalling and allosteric modulation.

Recent studies have identified the WRC as a key hub for signalling between the plasma membrane and actin in a variety of functions, elucidating various essential mechanisms of the WRC. It is widely accepted that in its basal state, the WRC is autoinhibited in the cytosol. Various upstream signals, such as ligand-binding proteins such as GTPases, inositol phospholipids, membrane receptors, and scaffolding proteins, as well as post-translational modifications such as phosphorylation and ubiquitination, frequently work together in the cell to relieve the inhibition. These signals cause WASP-family proteins to be recruited to the specific membrane regions where they will activate the Arp2/3 complex to promote actin polymerization (Abdul-Manan et al., 1999) (Rottner et al., 2021) (Fig. 4).

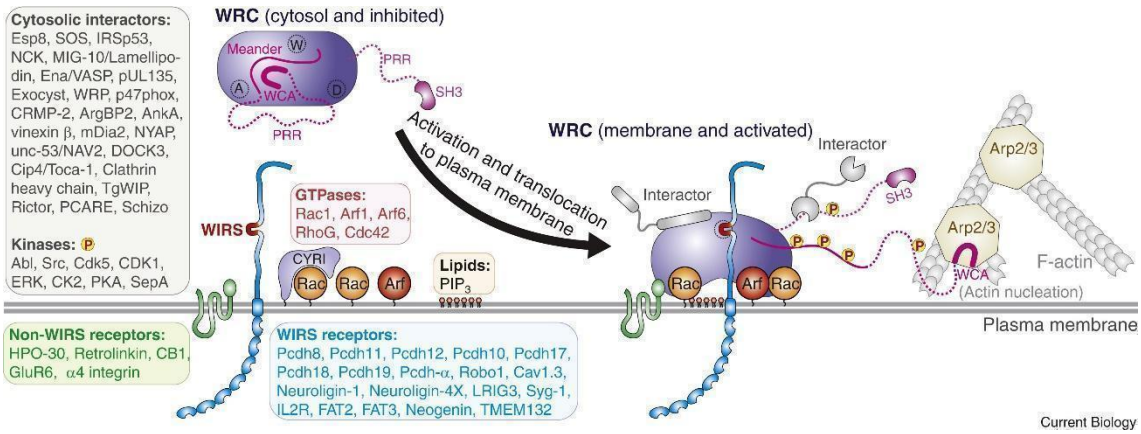

Figure 4

Simultaneous activation of the WRC and its migration to the plasma membrane by large groups of membrane ligands. This results in the release of the WCA, which then binds to the Arp2/3 complex to promote actin nucleation and the generation of branching actin networks. From (Rottner et al., 2021).

The WASP-family member WAVE exists exclusively in a 400-kDa, hetero-pentameric assembly named the WAVE Regulatory Complex (WRC) (Rottner et al., 2021). The WRC, which is essential to the majority of eukaryotic organisms, is crucial for stimulating actin polymerization at plasma membranes and creating lamellipodia, sheet-like membrane protrusions that are typically observed

at the leading edge of migrating cells (Alekhina et al., 2017). When WRC is in a basal state, it is auto-inhibited (Z. Chen et al., 2010). The overall structural organisation and the inhibition mechanism were disclosed by previous crystal structures of a minimum, inhibited WRC (Z. Chen et al., 2010).

The majority of eukaryotic taxa, such as mammals, plants, slime moulds, numerous protists, and single-celled algae, share five distinct protein components that constitute the WRC. Multicellular plants and vertebrates typically encode multiple orthologs for each subunit in their genomes (Fig. 5 from (Rottner et al., 2021)), including *SRA1/CYFIP1* (or its ortholog *PIR121/CYFIP2*), *NAP1/HEM2*, *ABI2*, and *HSPC300/BRICK1* as well as orthologs of *ABI1* and *ABI3/NESH* (or its orthologs *WAVE2* and *WAVE3*). Complex composed by SRA1, NAP1, ABI2, HSPC300, and WAVE1 is a major form in the human brain to the first crystal structure of the complex (Z. Chen et al., 2010).

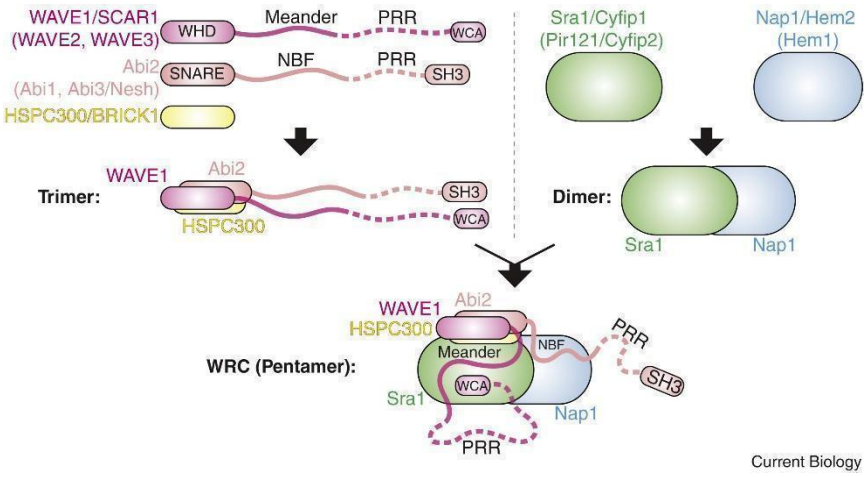

Figure 5

Schematic illustrating the *in vitro* biochemical reconstitution process used to assemble the WRC from five distinct subunits (Rottner et al., 2021).

Based on *in vitro* reconstitution and its crystal structures, the WRC may be easily divided into two parts: a larger elongated dimer of approximately ~10x10x20 nm generated by SRA1 and NAP1, and a smaller trimmer formed by WAVE1, ABI2, and HSPC300 (Fig. 5, top). A conserved motif known as the "meander" sequence, which is present in WAVE1, is around 100 amino acids (aa) long and meanders across the surface of SRA1 (Fig. 5, bottom). The WCA-binding site on SRA1 is made up of the meander region and a conserved surface, and it prevents the WCA from reaching the Arp2/3 complex (Z. Chen et al., 2010).

Biochemical and low-resolution cryo-EM studies suggested that WRC contains two unique RAC1-binding sites (Z. Chen et al., 2010). Both sites, which are separated by ~100 Å on the opposite ends of the WRC, were mapped on surfaces of SRA1. The site that is close to the WCA is known as the A site, while the site that is far from the WCA is known as the D site. Thus, the two sites permit the simultaneous binding of two separate RAC1 molecules with different affinities, with the D site binding being between 40 and 100 times stronger than the A site (B. Chen et al., 2017). Despite having a far lower affinity for RAC1 than the B site, in vivo research shows that the A site appears to have a more important role in promoting lamellipodia development (Schaks et al., 2018). Lamellipodia formation is almost completely terminated by mutating the A site, although its general morphology was affected by mutating the D site (Fig. 6 (Schaks et al., 2018)).

In a recent study, the structures of the WRC determined to ~3 Å resolutions by single-particle cryogenic-electron microscopy (cryo-EM) (Ding et al., 2022), better clarify the fundamental mechanism of WRC activation, an essential stage in Arp2/3 complex-mediated actin filament formation in cells.

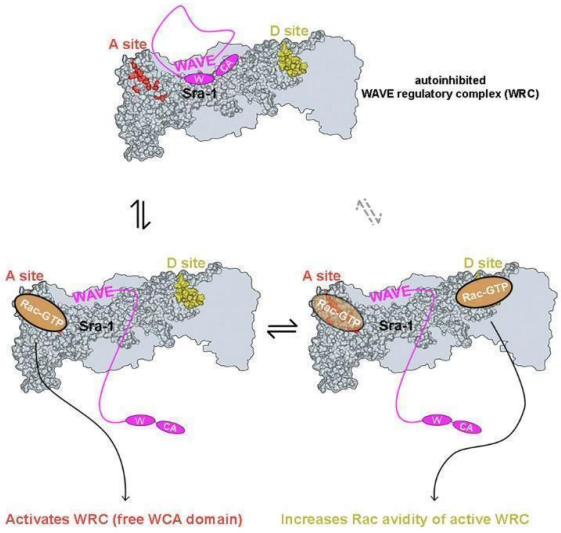

Figure 6

Schematic and cryo-EM density of WRCs show binding of one or two molecules of RAC1-GTP to A and D sites during complex activation process (Schaks et al., 2018).

Among multiple signals that have effect on WRC function (Alekhina et al., 2017; B. Chen et al., 2017), RAC signaling appears obligatory for lamellipodia formation. Physical interactions between RAC and WRC, mediated by SRA1/PIR121, are essential for this process (B. Chen et al., 2017). SRA1/PIR121 binds to both the W and C regions of WRC, locking the WCA domain of WAVE and inhibiting the activity of the complex. This explains why SRA1 and his orthologous PIR121 are

fundamental in several stages of WRC function. In a 2001 study, Schaks and colleagues engineered B16-F1-derived cell lines to destroy two mouse genes that code for *Sra-1* (*Cyfip1*) and *Pir121* (*Cyfip2*), using CRISPR/Cas9, demonstrating the crucial role of these WRC's subunits in the development of lamellipodia and membrane ruffling (Schaks et al., 2018).

1.2 Cytoplasmic FMRP interacting protein 1/2 (CYFIP1/2)

In 1997 a new target for the small GTPase RAC1 was identified in the bovine brain lysate by Kobayashi and colleagues. This 140 kDa protein named SRA-1, (specifically RAC1-associated protein) was also discovered to be a direct F-actin interactor (Kobayashi et al., 1998). Two years later, during a screening to identify possible new p53 target genes, a 140 kDa protein named PIR121 was identified (Saller et al., 1999). It was later revealed that *SRA-1* and *PIR121* are translated by an evolutionarily conserved family of orthologous genes.

Schenck and colleagues in 2001 reported the identification of two proteins that interact with Fragile X Messenger Ribonucleoprotein (FMRP). These proteins, termed Cytoplasmic FMRP Interacting Protein 1 and 2 (CYFIP1 and CYFIP2) (Schenck et al., 2001) are members of a highly conserved protein family in humans. They are distributed in an identical pattern in the cytoplasm and show colocalization with FMRP and ribosomes. It has been later shown that CYFIP1 and CYFIP2 are Sra-1 and PIR121, respectively.

The CYFIP1 and CYFIP2 proteins are approximately 145 kDa, and they share 88% identity and 95% similarity. These two proteins are highly conserved in several organisms (Zhang et al., 2018), and they share 99% identity with their orthologs in mice (Schenck et al., 2001).

1.2.1 CYFIP1

Cytoplasmic FMR1-interacting protein 1 (CYFIP1, SRA-1, KIAA0068, SHYC or P140SRA-1) is a protein coding gene located on chromosome 15q11.2. It is composed of 34 exons and might encode 3 isoforms produced by alternative splicing (UniProtKB Database, Q7L576). CYFIP1 protein is a 1253 amino acid long protein with a low tissue specificity expression rate (0.15 Tau specificity score RNA (Yanai et al., 2005)).

CYFIP1 was identified as a protein that interacted with Rac family small GTPase 1 (RAC1), a Rho small GTPase (Kobayashi et al., 1998), involved in a variety of biological functions (Abo et al., 1991; Guo et al., 2008; S. K. Kim, 2000) including actin filament rearrangement (Ridley et al., 1992). CYFIP1 is one essential component of the WAVE Regulatory Complex (WRC), a constitutively assembled pentameric complex (Takenawa & Suetsugu, 2007). RAC-GTP recruits and activates the WRC to the cell periphery. The Arp2/3 complex is activated by this complex, which also plays a role in the kinetics of actin cytoskeleton development (Campellone & Welch, 2010). Additionally, CYFIP1 interacts with FMRP (Schenck et al., 2001), a protein linked to the fragile X syndrome (FXS) (Verkerk et al., 1991). Loss of FMRP in FXS patients causes mental impairment and intellectual disability associated with the autism spectrum (Bagni & Oostra, 2013). CYFIP1 interacts with FMRP but not with Fragile X related protein 1 or 2 (FXR1P or FXR2P), two proteins that are related to FMRP (Schenck et al., 2001). Additionally, FMRP affects how several proteins regulate cytoskeletal reorganisation (Michaelsen-Preusse et al., 2018).

Napoli and collaborators demonstrated that CYFIP1 is an eIF4E-binding protein (4E-BP) that interacts with FMRP to form a post-transcriptional regulatory complex at the synaptic level. This complex inhibits the expression of FMRP target mRNAs, including MAP1B, ARC, and CaMKII. The FMRP target mRNAs are released for translation when synaptic stimulation causes CYFIP1 to separate from eIF4E (Napoli et al., 2008). De Rubeis and colleagues showed that CYFIP1's binding to the WRC contributes to the regulation of actin cytoskeleton at dendritic spines. The conformational swing of CYFIP1 from a globular to a planar form, which causes CYFIP1 to dissociate from eIF4E and facilitates the binding of NCKAP1 and the subsequent formation of WRC. This dynamic between the two complexes is controlled by RAC1 (De Rubeis et al., 2013).

Recent findings demonstrate the function of CYFIP1 in the NOTCH signalling pathway (Dziunycz et al., 2017; Habela et al., 2020). Because NOTCH is a key player in the balance between symmetrical and asymmetrical division in neural stem cells (Contreras et al., 2018; Egger et al., 2010), CYFIP1 expression seems to have a role in neural development processes.

1.2.2 CYFIP2

Cytoplasmic FMR1-interacting protein 2 (*CYFIP2*, *KIAA1168* or *PIR121*; NC_000005.10) is a protein coding gene located on chromosome 5q33.3 and might encode four isoforms (UniProtKB Database, Q96F07). CYFIP2 protein is a 1253 amino acid long protein and is highly conserved

sharing 99% sequence identity to the mouse protein (Schenck et al., 2001). It is expressed mainly in brain tissues, white blood cells and the kidney (Su et al., 2004).

In 2001, Schenck and colleagues showed that CYFIP2 and his orthologous CYFIP1 were FMRP interactors. Whereas CYFIP2 also interacts with the FMRP-related proteins FXR1P/2P, CYFIP1 interacts exclusively with FMRP. The FMRP-CYFIP interaction involves the FMRP domain that also mediates homo- and heteromerization, suggesting a possible competition between interactions with CYFIP and associations among the FXR proteins (Schenck et al., 2001).

Napoli and collaborators proposed a possible function of CYFIP2 in regulating FMRP target mRNA as described for CYFIP1 due to a conservation of the C-terminus eIF4E-binding domain (Napoli et al., 2008). CYFIP2 has been immunoprecipitated with eIF4E in rat primary cortical neurons, indicating their connection (Contreras et al., 2018). Interestingly, in the synaptosomes obtained from mice with *Cyfip2* heterozygous mutations, the expression levels of several FMRP targets, including APP and CaMKII, are normal (Han et al., 2015). In contrast, Tiwari and colleagues demonstrated an upregulation of APP and CaMKII proteins in hippocampus synaptosomes from *Cyfip2*$^{+/-}$ mice that was not followed by an increase in their mRNA levels, indicating that this alteration happened through post-transcriptional regulation (Tiwari et al., 2016). The genetic background of the animals in the experiments may be the cause of these variations; whereas Han and collaborators' study employed the C56BL/6 J lineage, Tiwari's study used the C56BL/6 N lineage. The *Cyfip2* gene in this last lineage is known to have a point mutation that has already been found to decrease *Cyfip2* function and to be linked to behavioural disorders (Bryant et al., 2008). In 2013, Kumar and colleagues, while trying to understand the genetic causes of phenotypic differences between C57BL/6N and C57BL/6J in a response to cocaine and methamphetamine, mapped a single causative locus and identified a nonsynonymous mutation of serine to phenylalanine (S968F) in *Cyfip2* as the causative variant (Kumar et al., 2013). The S968F mutation destabilised CYFIP2 reducing the protein's relative half-life. Deletion of the C57BL/6N mutant allele leads to acute and sensitised cocaine-response phenotypes. Dendritic spine morphology of medium spiny neurons in the nucleus accumbens of C57BL/6N, significantly decreased with a deficit in excitatory glutamatergic signalling prediction. It is unclear how this mutation affects CYFIP2's interaction with its partners, particularly FMRP, hence this variation may have an influence on the findings from various animal lineages. The interaction of CYFIP2 with 25 additional RNA metabolism-related proteins in mouse brains has recently been characterised. These proteins include those involved in mRNA processing and the miRNA pathway, such as Pumilio1 (PUM1) and Argonaute2 (AGO2) (Lee et al., 2020).

Additionally, it has been suggested that circCYFIP2, a sense-overlapping circular RNA spliced from the *CYFIP2* transcript, acts as a sponge for miR-1205. This miRNA controls the expression of E2F1, a protein that has been previously identified as being overexpressed in tumours. The circCYFIP2-miR-1205-E3F1 pathway is implicated in gastric cancer cell migration and proliferation, which raises the possibility that circCYFIP2 functions as a biological marker for the illness (Lin et al., 2020).

In 2007, Jackson and colleagues discovered that the *CYFIP2* promoter contains a p53-responsive element that confers p53 binding as well as transcriptional activation. Inducible expression of *CYFIP2* is sufficient for caspase activation and cellular apoptosis, reminiscent of p53 activation (Jackson et al., 2007). Once p53 expression is down regulated in many types of cancer (Ozaki & Nakagawara, 2011), *CYFIP2* expression may be impacted. To determine the molecular function of *CYFIP2* in posttranscriptional regulation and cancer development, more research is required.

Moreover, Mayne and collaborators analysed CD4+ cells in patients with multiple sclerosis, a disease in which T cell adhesion is crucial. In these cells, CYFIP2 expression is increased. High concentrations of CYFIP2 may help T cells adhere since the protein regulates the WRC complex. Healthy T cells overexpressing CYFIP2 exhibit much higher adhesion when compared to the control. Furthermore, CYFIP2 reduction in CD4+ cells from MS patients reduces adhesion. (Mayne et al., 2004).

1.2.3 CYFIP family and neural disorders

Understand the pathophysiological differences between CYFIP orthologous proteins, it is crucial to explain the exact processes driving the in vivo differences between CYFIP1 and CYFIP2.

Abekhoukh and Bardoni proposed that the function and role of these two proteins in neuronal maturation are similar (Abekhoukh & Bardoni, 2014). Recently, Schaks and collaborators showed that mutations described for CYFIP2 can be transferred to CYFIP1 and impact on the actin dynamics driven by WRC (Schaks et al., 2020). This result points to a conservative function of the CYFIP family concerning the regulatory complex. Moreover, other studies have suggested that they may perform some different biological functions (Zhang et al., 2018). Cioni and collaborators emphasised the significance of both CYFIP proteins in brain development. *cyfip1* and *cyfip2* knockdown affects axon sorting using retinal glial cells (RGCs) from zebrafish embryos and in vivo time-lapse imaging of the Xenopus brain. They discovered nonredundant functions of the proteins

with CYFIP1 involved in axon extension and CYFIP2 involved in proper axon sorting (Cioni et al., 2018). CYFIP1 and CYFIP2 genetic variations have been linked to a variety of brain disorders. Autism spectrum disorders, intellectual disability, and schizophrenia have been linked to deletions and duplications of the chromosomal region that contains *CYFIP1* (15q11-13) (Abekhoukh & Bardoni, 2014; Bagni & Zukin, 2019). On the other hand, individuals with early-onset epileptic encephalopathy, which is characterised by developmental delay and seizures, have de novo *CYFIP2* mutations, according to current whole-exome and genome sequencing studies (Nakashima et al., 2018; Peng et al., 2018; Zweier et al., 2019). Due to contradictory results, the functions of the CYFIP family at the molecular level need to be better elucidated to identify the roles of *CYFIP1/2* in neural development and the impact of *CYFIP1/2* dysfunctions on neural disorders.

CYFIP1 is linked to a variety of behavioural and cognitive impairments, including schizophrenia (Domínguez-Iturza et al., 2019), autism spectrum disorders (Noroozi et al., 2018), and intellectual disability (ID) [4883502]. Individuals with schizophrenia had lower levels of *CYFIP1* mRNA in their peripheral blood, whereas patients with epilepsy have higher levels (Sayad et al., 2018). Furthermore, *CYFIP1* cooperates with Neuroligin3 to modulate hyperactivity. Oguro-Ando et al. demonstrated that *CYFIP1* is overexpressed in lymphoblastoid cell lines and the temporal cortex of ASD patients with duplication at 15q11–13. They also discovered elevated levels of mTOR and phosphorylation of S6 (a downstream effector of mTOR) in the brain tissue of these patients, indicating a role for *CYFIP1* in the regulation of mTOR signalling associated with ASD (Oguro-Ando et al., 2015). In lymphocytes and the brain of FXS patients, there is a reduction in *CYFIP1* mRNA levels and an increase in the phosphorylation of two mTOR effectors, S6K1 and AKT (Hoeffer et al., 2012). These results indicate that FMRP may influence the effects of *CYFIP1* in the regulation of mTOR signalling. Additionally, Silva and co-workers demonstrated how *CYFIP1* is also involved in oligodendrocyte maturation. *CYFIP1* haploinsufficient mice exhibit altered brain white matter, reduced myelin thickness, and reduced expression of oligodendrocyte maturation markers (Silva et al., 2019). Since learning and behavioural plasticity depend on adequate myelination, *CYFIP1* can have a role in both neuronal and glial processes. In addition to have a link to myelination, Fricano-Kluger et al. demonstrated that mice overexpressing *Cyfip1* in the amygdala also had learning deficiencies and enhanced fear conditioning, comorbidities connected to some cases of ASD (Fricano-Kugler et al., 2019).

Despite some evidence suggesting that *CYFIP2* downregulation may not be linked to abnormal social and repetitive behaviour (Tiwari et al., 2016), Han et al. demonstrated that alterations in *CYFIP2* have been linked to behavioural and cognitive impairments. While *Cyfip2 KO* die at

embryonic stage, C56BL/6J mice heterozygous for *Cyfip2* exhibit some fragile X-like behaviours. These effects are strengthened in mice double knockout *Fmr1*$^{+/-}$, *Cyfip2*$^{+/-}$ (Han et al., 2015). Dendritic spines were altered in *Cyfip2*$^{+/-}$ cortex, and the dendritic spine phenotype of *Fmr1*$^{-/y}$ cortex was aggravated in *Fmr1*$^{-/y}$ *Cyfip2*$^{+/-}$ double-mutant mice. In addition to the spine changes at basal state, metabotropic glutamate receptor (mGluR)-induced dendritic spine regulation was impaired in *Cyfip2*$^{+/-}$ cortical neurons. These data suggest that misregulation of CYFIP2 might impair FMRP function and contribute to the neurobehavioral phenotypes of FXS (Han et al., 2015). However, the mechanistic link between CYFIP2 impairment and FMRP function is still to be investigated.

Cyfip2 is also correlated with binge eating disorder in mice. Animals with the CYFIP2 S968F mutation exhibit compulsive eating behaviours, which may be related to myelination genes being downregulated (Kirkpatrick et al., 2017). CYFIP2 has also been linked to Alzheimer's disease. Ghosh and co-workers recently demonstrated that *Cyfip2*$^{+/-}$ aged mice exhibit Aβ accumulation in the brain, gliosis, synapse loss, and memory impairment (Ghosh et al., 2020). A decrease in CYFIP2 expression in neuronal cells sets off several pathological changes, including the hyperphosphorylation of the TAU protein, the development of amyloid plaques, and memory loss (Tiwari et al., 2016). TAU, a microtubule-stabilising protein, can mislocalise to dendritic spines as a result of hyperphosphorylation (Hoover et al., 2010). Reduction in CYFIP2 levels lead to an increase in TAU phosphorylation that causes a TAU dislocation to dendritic spines with consequent deficits in microtubule integrity and organelle trafficking. This series of events may be the cause of the decrease in mitochondria numbers in the presynaptic region in the cortex of adult *Cyfip2* heterozygous mice (G. H. Kim et al., 2020).

Recently, de novo missense mutations in *CYFIP2* have been associated to developmental and epileptic encephalopathy-65 (DEE65; MIM: 618008), characterised by severe to profound psychomotor developmental delay, onset of intractable seizures usually within the first months or years of life and mild facial dysmorphism. Three de novo *CYFIP2* variants were found in four unrelated individuals with early-onset epileptic encephalopathy, all affecting the arginine at position 87 (Nakashima et al., 2018) (Fig. 7). Moreover, twelve independent patients harbouring eight distinct de novo variants in *CYFIP2* broaden the molecular and clinical spectrum of this novel *CYFIP2*-related neurodevelopmental disorder. The patients shared a phenotype of ID, seizures, and muscular hypotonia (Zweier et al., 2019). Despite the large spacing in the primary structure, the variants spatially cluster in the tertiary structure and are all predicted to weaken the interaction with WAVE1 of the actin polymerization regulating WRC-complex. Very recently, nineteen newly

identified patients with mild and severe phenotype, harbouring two previously described and eleven novel disease-associated missense variants were reported (Begemann et al., 2021).

Therefore, further research is needed to understand the crucial function that CYFIP2 plays in the development of neurodegenerative disorders.

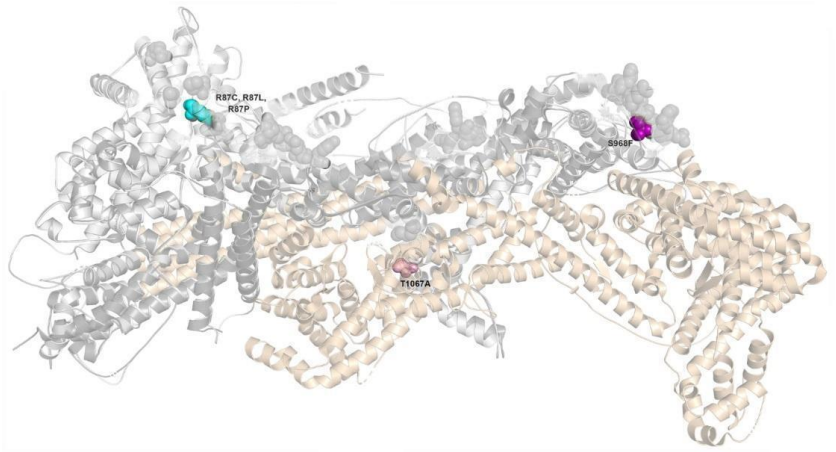

Figure 7

Model of CYFIP1/2 protein (dark grey/light grey) interacting in the WRC complex (wheat). The model of CYFIP2 was constructed using Modeller and the CYFIP1 structure as a template (PDB: 3P8C, CYFIP1 shares 95% similarity with CYFIP2). Other WRC chains were obtained from PDB structure 3P8C. Spheres emphasise the regions where reported mutations in CYFIP proteins lead to biological effects. Mutations reported in CYFIP2: the R87C, R87P, and R87L promote weaker interaction between CYFIP and the VCA domain of WAVE (cyan). The S968F mutation is correlated to protein destabilisation (purple). The T1067A mutation decreased the density of stubby spines in cultured hippocampal neurons (pink). Modify from (Biembengut et al., 2021).

1.2.4 *CYFIP2* RNA editing

Interestingly, in an article published in a 2005 Levanon and colleagues found that *CYFIP2* transcript undergoes RNA editing (Levanon et al., 2005), a post-transcriptional mechanism catalysed by Adenosine Deaminase Acting on RNA (ADAR) enzymes, that leads adenosine (A) to inosine (I) deamination. When this reaction occurs in the coding sequences (CDS), it causes an amino acid substitution that contributes to increase the proteomic complexity of the cells (Orlandi et al., 2012). The *CYFIP2* editing results in a K/E substitution at amino acid 320 in both human and mouse proteins.

Human embryonic stem cells and foetal brains do not exhibit any evidence of *CYFIP2* RNA editing like the adult brain (Shtrichman et al., 2012). It is interesting to note that Nicholas and colleagues

found that *CYFIP2* editing levels decline with ageing in the adult human brain (Nicholas et al., 2010). In addition, Bonini and colleagues demonstrated that cortical rat cells treated with glutamate, an essential excitatory neurotransmitter, had lower ADAR2 expression and self-editing, which impacts *CYFIP2* RNA editing levels. How this affects brain functioning is still unknown. (Bonini et al., 2015).

These data indicate together that *CYFIP2* RNA editing is critical for brain development and maturation, and more research is required to fully understand this link.

1.3 RNA editing

All cells in the human body have the same genetic content but different cell types have distinct peculiar roles to maintain the right physiology. Cells accomplish their molecular complexity through a number of methods, including transcriptional control, mRNA processing and post-translational protein changes. One of the methods that helps to increase the biological information from a single transcript in terms of RNA processing is alternative splicing. Additional systems produce a variety of transcriptomes from a static genome. The co-transcriptional event known as "RNA editing" is one of the most explored processes that takes place at the RNA level. (Bajad et al., 2017).

According to Keegan and collaborators, two types of RNA editing occur in mammals and both of them involve the deamination of a specific nucleotide in a double strand RNA (dsRNA), or the hydrolysis of an amino group in a particular RNA base (Keegan et al., 2001). The results are the conversion of a cytosine (C) into a uracil (U) or an adenosine (A) into inosine (I). Today the term “RNA editing” refers to any RNA site-specific substitution. RNA editing can modify the primary structure of the proteins by introducing single amino acid substitutions, new start and stop codons or by modifying splicing sites. Furthermore, it can also affect RNA stability by modifying the Untranslated Regions (UTRs) (Daniel et al., 2015; Nishikura, 2016). In addition to affecting RNA processing, coding, and gene expression (Fig. 8, right), RNA editing also regulates the antiviral response to double stranded RNAs, which are a key characteristic of viral infections. The discovery of numerous regulatory levels through which ADARs can influence antiviral programmes is one of the most intriguing results of recent improvements in our understanding of ADAR enzymes (Fig. 8, left) (Mannion et al., 2014).

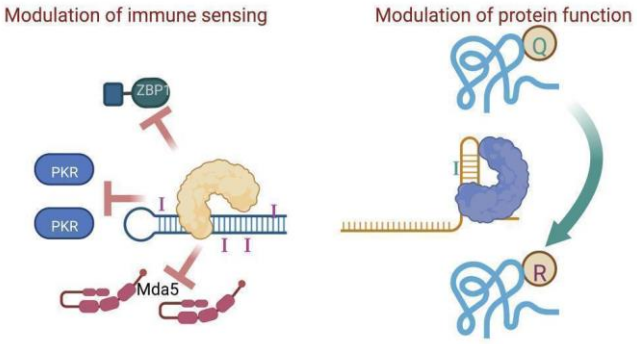

Figure 8

Different functions of ADAR enzymes. From (Goldeck et al., 2022)

1.3.1 A to I RNA editing

The most common type of RNA editing in mammals is called an A to I editing (Fig. 9, top) (Maas et al., 2003). The majority of human genes contain Alu sequences, which contain about 100 million adenosine (A)- to-inosine (I) editing events (Bazak et al., 2014).If the nucleotide being edited is within a coding sequence, the ribosomes will interpret the inosine as a guanosine, altering the meaning of the RNA codon (Fig. 9, bottom).

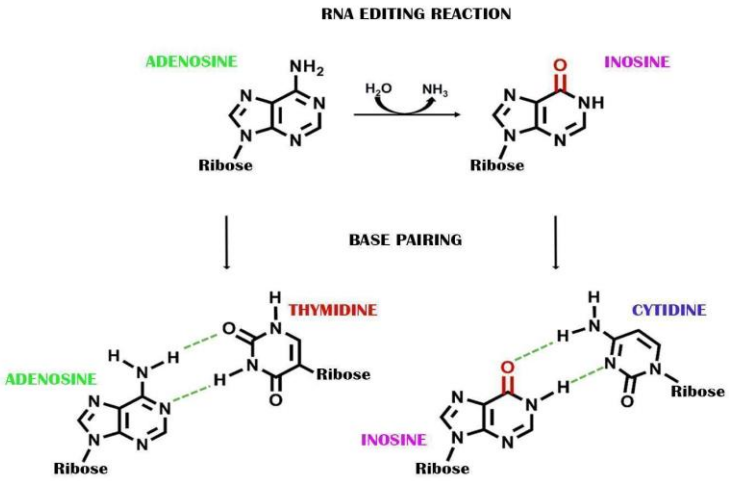

Figure 9

Schematic illustration of the generation and base pairing of Inosine (I). Adenosine in RNA is deaminated to generate Inosine through hydrolytic deamination of the amino group at the C6 position of adenosine (top). Adenosine base pairs with thymidine, while Inosine base pairs with cytidine.

During the editing reaction, the primary transcript undergoes a double strand conformation, due to complementary sequences located between the exon with the editing site and the downstream intron and specifies the Editing Complementary Sequence (ECS).

Adenosine Deaminases Acting on RNA (ADAR), which are highly conserved across metazoans, are the enzymes that catalyse the RNA editing reaction. The ADAR family in mammals consists of three members: ADAR1, ADAR2, and ADAR3. They function as homodimers (Chilibeck et al., 2006) and exhibit a variety of activities and cellular localizations, primarily nuclear and nucleolar. While ADAR1 and ADAR2 are active enzymes, ADAR3 is largely expressed at low levels in brain areas and has no enzymatic activity (Barbon & Magri, 2020; Orlandi et al., 2012). The 110-kDa (p110) constitutive isoform of ADAR1 and the interferon-inducible (p150) isoform are two splicing variants of the protein (Filippini et al., 2018). The two most prevalent ADAR2 splicing isoforms are the short ADAR2S (ADAR2a) and the long ADAR2L (ADAR2b), which differ due to alternative splicing on the deaminase domain and result in different functional activity (Filippini et al., 2018; Gerber et al., 1997).

Millions of sites in the mammalian transcriptome are edited by ADAR enzymes. Most of them are present in non-coding sequences, such as intronic retrotransposons like ALU-inverted repeats, 3′UTRs, and 5′UTRs (Daniel et al., 2015). Although there is some overlap between the target sites of the two enzymes, ADAR1 typically mediates RNA editing in repetitive regions, such as ALU sequences, whereas ADAR2 preferentially performs RNA editing at coding sites (specifically re-coding sites). Until now, 2.5 million editing sites have been discovered.

1.3.2 A to I RNA editing functions

In double-stranded or structured RNAs, ADAR enzymes modify adenosines (A) to inosines (I). When compared to the original adenosine, inosines have a different base pairing potential due to the lack of its amino group. In consequence, inosines can base pair with uracil or adenine but prefer to base pair with cytosines. This process can have an impact on protein decoding at the ribosome (re-coding editing), over on the folding of RNAs and the proteins that may interact with these new edited RNA molecules. Consequently, an A to I exchange can also affect RNA processing and turnover (Brümmer et al., 2017; Nishikura, 2010). All of these events will alter gene expression, which may also have an impact on cellular and physiological processes (Fig. 9, right).

Re-coding editing events predominantly depend on ADAR2, whose expression is mostly restricted in specific cell types or tissues. Consequently, the resulting regulations can be found in a subset of tissues (Gabay et al., 2022). Numerous re-coding sites impact on transcripts crucial for neuronal functions and are phylogenetically conserved (Behm & Öhman, 2016). For instance, it has been discovered that RNA editing of re-coding sites affects the permeability of ion channels and responses to excitatory neurotransmitters (Rosenthal & Seeburg, 2012). Additionally, research conducted *in vitro* and *in vivo* have demonstrated that these locations are tightly controlled throughout development (Orlandi et al., 2011; Wahlstedt et al., 2009).

Since the participation of RNA editing in the proper cellular processes such as neurodevelopment and brain function, the role of RNA editing in psychiatric disorders has gained an increasing interest. Major depression, Alzheimer's disease (Gardner et al., 2019; Wahlstedt et al., 2009), amyotrophic lateral sclerosis (Moore et al., 2019), schizophrenia (Breen et al., 2019), and autism (Eran et al., 2013; Tran et al., 2019) are among the neurological and psychiatric illnesses for which RNA editing has now been documented. How widespread altered RNA editing is in the brains of psychiatric patients is still unknown.

In a 2005 study, using comparative genomics and expressed sequence analysis, Levanon and colleagues discovered four more candidate human substrates for ADAR-mediated editing: *FLNA*, *BLCAP*, *CYFIP2*, and *IGFBP7*. Interestingly, only two of these substrates are prominently expressed in the CNS and appear to be crucial for healthy nervous system function. None of these substrates encode for a receptor protein (Levanon et al., 2005).

2 AIMS

A variety of eukaryotic cell functions, including cell migration and vesicle trafficking, are driven by the dynamic rearrangement of the actin cytoskeleton. Dysregulation of this structure is strongly linked to a number of pathologies, including cancer, immunological deficiencies, and neurological disorders. Actin cytoskeleton is also an essential factor in determining the shape and function of cells. In neurons, one of the most remarkable examples of cellular polarisation, the coordination of actin filaments dynamics is crucial to the development, maturation, and function. Moreover, the remodelling of the underlying actin cytoskeleton is a large determinant in how dendritic spine size and shape vary in relation to excitatory synapses functions. Spine development, plasticity and synaptic function all depend on actin dynamics. This process is one of the bases underlying synaptic plasticity processes (Citri & Malenka, 2008). In addition to synaptic impacts, regulation of actin cytoskeleton dynamics is essential for the development of brain circuits complexity, modifying and guiding the extension of axonal projections from neurons to their specific destination for synaptic connections.

Cytoplasmic FMRP Interacting Protein 2 (CYFIP2) is a component of Wave Regulatory Complex (WRC), one of the most important players that regulate cellular actin dynamics. Interestingly, *CYFIP2* transcript undergoes RNA editing, an epi-transcriptomic mechanism catalysed by ADAR enzymes, that leads adenosine (A) to inosine (I) deamination. *CYFIP2* editing results in a K/E substitution at amino acid 320 in both human and mouse proteins. The functional meaning of this regulation is still unknown. In this study, we aim at investigating the potential implication of this process related to actin dynamics during cell migration, axon development and synaptogenesis in neural cells. Understanding the role of *CYFIP2* RNA editing substitution would be fundamental for further analysis in normal and pathological conditions.

3 MATERIALS & METHODS

3.1 Protein model prediction of *CYFIP2* K/E 320 RNA Editing

Dynamut2 http://biosig.unimelb.edu.au/dynamut2/ (Rodrigues et al., 2021) were used to analyse and predict protein stability and flexibility changes after K→E substitution following the RNA editing process. DynaMut2 is a web server that combines Normal Mode Analysis (NMA) methods to capture protein motion and graph-based signatures to represent the *wild-type* environment to investigate the effects of single and multiple point mutations on protein stability and dynamics. For single-point mutations, DynaMut2 predict variations in Gibbs Free Energy (ΔΔG) and in melting temperature (ΔTm).Two distinct states of the complex derived from Cryo-EM technique were investigated: one without Rac1 bounded represent the constitutively inactive form (PDB 7USC) and one with Rac1 molecules simultaneously bound to both the A and D sites (PDB 7USE) represent the active form of complex (Ding et al., 2022).

3.2 Analysis of CYFIP2 K/E amino acid conservation during evolution

To analyse the conservation rate of CYFIP2 protein in different species, we aligned protein similar to CYFIP2 using NCBI Orthologs (https://www.ncbi.nlm.nih.gov/gene/26999/ortholog/?term=CYFIP2). A number of 438 proteins for jawed vertebrates (Gnathostomata) are processed, aligned protein sequences using Constraint-based Multiple Alignment Tool COBALT (https://www.ncbi.nlm.nih.gov/tools/cobalt/cobalt.cgi).

3.3 Cell cultures

3.3.1 HEK293T

Cells were cultured at 37°C and 5% CO2 in DMEM medium (Invitrogen) supplemented with 10% of heat-inactivated fetal bovine serum (FBS), 30 U/mL Penicillin, 30 mg/mL Streptomycin (Sigma-Aldrich®), 1% minimum Eagle's medium nonessential amino acids (Gibco™, Thermo Fisher

Scientific), 1 mM sodium pyruvate (Gibco™, Thermo Fisher Scientific). Cells were split at approximately 80% confluency.

3.3.2 SH-SY5Y

The human neuroblastoma SH-SY5Y cell line was purchased from the American Tissue Culture Collection (ATCC™, CRL2266). SH-SY5Y *CYFIP2-KO* was produced in our laboratory using CRISPR-Cas9 technology. Both cell lines will be grown in 1:1 mixture of Ham's F12 Nutrient Mix (#11765054 Gibco™, Thermo Fisher Scientific) and Dulbecco's modified Eagle's medium, (DMEM, #D6429, Sigma-Aldrich®) containing high glucose (4500 mg/L), L-glutamine (4 mM) and sodium pyruvate (1 mM). This medium was supplemented with 10% (v/v) heat-inactivated fetal bovine serum (FBS, #10270, Gibco™) and 1% antibiotic antimycotic solution (#A5955, Sigma-Aldrich®). Cells will be cultivated in T175 flasks at 37 °C with 5% CO2 at saturated humidity and kept below ATCC passage + 15 to avoid cell senescence.

3.3.3 Primary hippocampal neurons

Primary hippocampal neurons were prepared as described in Goslin and Banker, (Schacher, 1992). Briefly, hippocampi from embryonic day 16.5 were dissociated mechanically and neurons were resuspended in Neurobasal™ medium supplemented with B27 (Gibco™, Thermo Fisher Scientific) containing 30 U/ml Penicillin, 30 mg/mL Streptomycin (Sigma-Aldrich®), 0.75 mM Glutamax (Gibco™, Thermo Fisher Scientific) and 0.75 mM L-Glutamine (Gibco™, Thermo Fisher Scientific). Depending on following experiments, neurons were seeded 100.000 cells/ 2 cm2 on 0.1 mg/mL Poly-D-Lysine-coated glass coverslip or 250.000 cells/ 10 cm2 in 0.02 mg/ml Poly-D-Lysine-coated 6-multiwell plates and maintained at 37°C under a 5% CO2 humid atmosphere. Three days after seeding, half of the medium was replaced with 24 hours-astrocyte-conditioned medium. After, half of the medium was changed every seven days up to a maximum of four weeks.

3.3.4 SH-SY5Y differentiation

To differentiate SH-SY5Y cells, we use a well-established model of neuronal differentiation based on the application of a two-step retinoic acid (RA) and brain-derived neurotrophic factor (BDNF) protocol (Hromadkova et al., 2020). In brief, cells were seeded at a density of 1×10^4 cells/cm^2. For

confocal microscopy, poly-d-lysine pre-coated 8-well slides were used. Cells were seeded at day 0 and growth in RALS medium (DMEM/F12 1:1; 3% FBS; P/S; 4 mM L-glutamine; RA 10 μM) was changed twice each 48 h. The culture medium was replaced with RANBB medium (NeuroBasal medium; B27; P/S; 4 mM L-glutamine; RA 10 μM; BDNF 50 ng/ml). Every two days, the media was changed, and the cells were then considered differentiated.

3.3.5 Treatment of neuronal cultures

Hippocampal neuronal cells at DIV 14 were chronically treated with 10 μM Glutamate (Sigma-Aldrich®) (Qian et al., 2011). After 24 hr of treatment, cells were harvested, and total RNA was extracted to carry out an RNA editing quantification of *CYFIP2* transcript. Each experiment was performed using 3 independent preparations of DIV14 neurons.

3.4 Molecular biology techniques

3.4.1 Total RNA Isolation

Neuronal cultures at different DIV or cell cultures growing in adhesion were washed with RNAse-Free PBS and mechanically harvested in 1 mL of TRIzol™ (Thermo Fisher Scientific). An equal amount of 100% ethanol was added to each sample lysed in TRIzol™ and mixed thoroughly. The mix was transferred into a *Zymo-Spin*™ Column and centrifuged at 12,000 g for 30" to ensure RNA binding to the column. The column was then incubated with 80 μL of DNase I 15' at RT for digesting DNA. After two washes with *Direct-zol*™ *RNA* PreWash (12,000 g for 30'') and one wash with *RNA Wash Buffer* (12,000 g for 30''), the RNA bound to the column was eluted with 40 μL of Dnase/Rnase-Free water. The concentration of the eluted RNA was measured on a Nanodrop™ ND-1000 Spectrophotometer (Thermo Fisher Scientific).

3.4.2 Reverse transcription

Total RNA was reverse transcribed using Moloney Murine Leukaemia Virus Reverse Transcriptase (M-MLV RT) (ThermoFisher Scientific). 1 μg of each template RNA was incubated with 0,3 μg/mL Random Primers (ThermoFisher Scientific), 10 mM dNTPs (ThermoFisher Scientific), 5X First

Strand Buffer (250 mM Tris-HCl (pH 8.3), 375 mM KCl, 15 mM Magnesium Chloride; ThermoFisher Scientific), 0,1 M DTT (ThermoFisher Scientific), 200U M-MLV RT (ThermoFisher Scientific), and water to a final volume of 20 µL at 37°C for 2 h followed by 10 minutes at 75°C to inactivate the enzyme.

3.4.3 cDNA amplification

To perform PCR reactions of the target genes, normalised amounts of the RT products was mixed with 12.5 µl of 2X DreamTaq™ Green PCR Master Mix (Thermo Scientific™) and 1 µl of each forward and reverse primer (25 pmol/µl), to a final volume of 25 µl. PCR reaction was performed using the recommended thermal cycling conditions outlined below: one denaturation step for 2 min at 95 °C, followed by the appropriate number of cycles with 30 s of denaturation at 95 °C, 20 s of primer annealing at 60 °C, 30 s of elongation at 72 °C following by a final extension of 1 min.The primers used to amplify the cDNA sequence subjected to the RNA editing process are listed in Table 1.

hCYFIP2 EF	GCCAAGAAGAGAATTAATCTTAGCAAAATTG
hCYFIP2 ER	ACTGGGGGCTGATGCTGCTCTG

Table 1

List of primers used to amplify the cDNA sequence subjected to the RNA editing process.

3.4.4 Sanger sequencing

The PCR reactions were purified through ExoSAP® according to the manufacturer's instructions. Briefly, 5µl of PCR were incubated with 1.5µl of ExoSAP mixture (1:2 ratio of exonuclease and shrimp alkaline phosphatase, SAP) for 15 min at 37°C and then the enzymes were inactivated for 15' min at 85°C. After PCR purification, the Sanger sequencing reaction were performed using Mastercycler Gradient (Eppendorf S.r.l.). The reaction mix is composed of: 1µl of terminator ready reaction mix; 1.5µl of dilution buffer, 1µl of 4 pmol/µl primer, 20ng of purified PCR and water until the final volume of 10µl is reached. The extension program is designed like this: 1 min at 95°C, followed by 25 cycles of repeated three steps made of 10 sec at 96°C, 5 sec at 55°C, 4 min at 60°C. After this process, another purification step is made with Performa® Dye Terminator removal (Edge

BioSystems) columns to eliminate all the excess of fluorescent terminator dye. Then, the samples are dried at 95°C, resuspended in formamide and denatured at 95°C for 3 min before being processed through SeqStudio™ Flex Genetic Analyzer (ThermoFisher Scientific). The primers used to sequencing the vector pRRLSIN.cPPT.PGK-hCYFIP2-HA.WPRE are displayed in table 2.

hCYFIP2 352 For	GAGGTCACCAAGCTCATGAAGTTCATG
hCYFIP2 427 Rev	GCCGCTTCACCTCGCTGCAGAA
hCYFIP2 1366 For	ATGATCAAAGGCCTGCAGGTGCTC
hCYFIP2 2331 For	ATCCTTGGACCAAGCTATCAGCCG
hCYFIP2 2891 For	ATGAGTATGGCTCCCCAGGGATC
hCYFIP2 3370 For	GTGGAGTTCCACCGGCTGTGGA
hCYFIP2-436 Rev	AAAGTCCTTCCTGCGCTCGG
hCYFIP2-1450 Rev	GTCACCTGGGCGAAGTCCT
hCYFIP2-2327 For	TAAATCCTTGGACCAAGCTATCAG
hCYFIP2-2853 For	ATAGAGGTGATGCCCAAGATATGC
hCYFIP2-3516 For	TTTGACCTGTTCGACTTCTGTTACCA

Table 2

List of primers used to sequence the vector pRRLSIN.cPPT.PGK-hCYFIP2-HA.WPRE.

3.5 RNA editing quantification

The editing levels for *CYFIP2* mRNA were quantified by sequence analysis as previously described (Barbon et al., 2003). Briefly, in the electropherogram obtained after real-time PCR (RT-PCR) and sequencing analysis of a pool of transcripts that might be edited or not, the nucleotide that undergoes the editing reaction appears as two overlapping peaks, A from unedited transcripts, and G from the edited ones. The editing level was calculated as a function of the ratio between the G peak area and the sum of A and G peaks areas (Fig. 10). The areas representing the amount of each nucleotide were quantified using Discovery Studio (DS) Gene 1.5 (Accelrys Inc., San Diego, CA, USA).

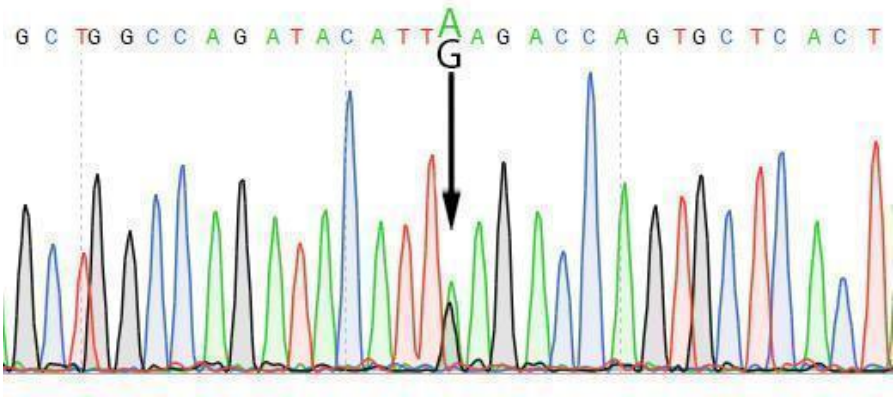

Figure 10

Detail of the electropherogram produced following Sanger sequencing of exon 10 of the *CYFIP2* transcript. The K/E editing site is represented by the overlapping of A and G peaks indicated by the arrow.

3.6 Cloning of human *CYFIP2* coding sequence

After total RNA purification from murine cortical tissue using RNeasy mini kit (Quiagen™), we perform a retrotranscription reaction (M-MLV Reverse Transcriptase, Invitrogen™). cDNA generated is used to amplify *CYFIP2* whole CDS through PCR reaction with Q5 High-Fidelity® DNA polymerase (New England Biolabs™) using a couple of primer shown in the Table 3.

hCYFIP2_AgeI_ATG_For	TTACCGGTCGCCACCATGACCACGCACGTCACCCTG
hCYFIP2_HA_TAA_SalI_Rev	ATTGTCGACTTAAGCGTAATCTGGAACATCGTATGGGTAGCAAGTGGTGGCCAAGG

Table 3

List of primers used to amplify the full length CDS of human *CYFIP2* transcript.

Primers contain respectively AgeI and SalI restriction site, which will use to insert the amplicon in to pRRLSIN.cPPT.PGK-GFP.WPRE Lentiviral vector (#12252 Addgene™ - Trono Lab). Reverse primers also contain sequence coding HA-TAG.

The enzymatic digestion of 1µg of CYFIP2 PCR product and pRRLSIN.cPPT.PGK-GFP.WPRE plasmid was carried out through SalI FastD 10 U/µl (Thermo Fisher Scientific) and AgeI 10 U/µl

(Thermo Fisher Scientific) in Buffer Orange (Thermo Fisher Scientific) for 3h at 37°C. The subsequent inactivation was accomplished for 10' at 65°C. Then 20µl of digestion product were dephosphorylated with the Shrimp Alkaline Phosphatase (SAP Invitrogen™) 30' at 37°C, followed by the enzyme inactivation 10' at 65°C. After the purification and gel quantification of the digestion products, the ligation reaction was set up in a volume of 20µl with a ratio 1:3 of empty vector (50ng) and *CYFIP2* insert DNA respectively, 1µl T4 DNA Ligase 5U/µl (Thermo Fisher Scientific) and T4 DNA Ligase Buffer 10×; the reaction mixture was maintained 1h at 22°C. Once obtained the ligation product, called pRRLSIN.cPPT.PGK-hCYFIP2-HA.WPRE (Fig. 11), the bacterial transformation was carried out using TOP10 bacteria strain (Thermo Fisher Scientific). After an overnight growth at 37°C on a LB-Agar plate under Carbenicillin selection, one CYFIP2 positive colony was selected for a subsequent MIDI-Prep preparation (MN™ kit) according to the manufacturer instructions. We perform a Sanger sequencing of plasmid DNA to confirm the absence of mutations within the generated sequence.

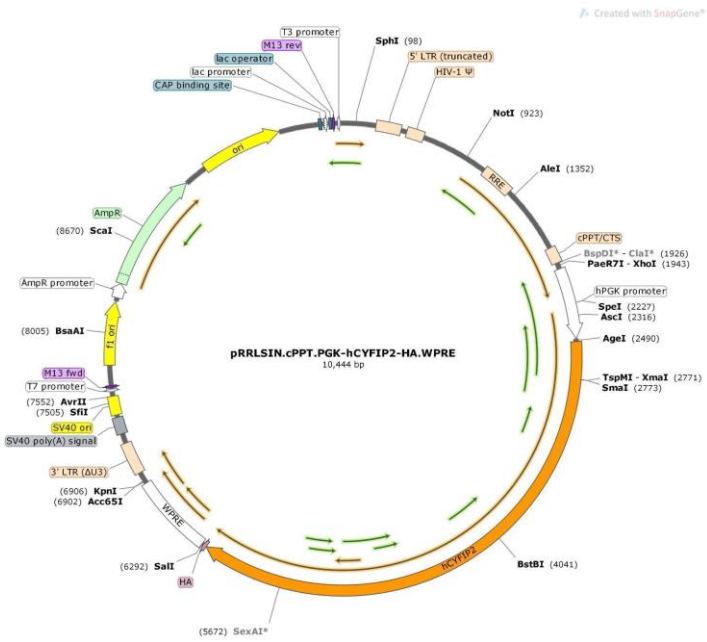

Figure 11

Lentiviral vector pRRLSIN.cPPT.PGK-hCYFIP2-HA.WPRE generated from pRRLSIN.cPPT.PGK-GFP.WPRE plasmid backbone (#12252 Addgene™ - Trono Lab). The insert consisting of the CDS of human CYFIP2 transcript (NM_001037333.3) is orange-highlighted.

3.7 *In vitro* mutagenesis

To generate an edited form of lentiviral CYFIP2 vector, we perform an *in vitro* mutagenesis reaction. Point-mutations can be introduced to plasmids using primers bearing the desired mutation, in a PCR protocol that amplifies the entire plasmid template. The parent template is removed using a

methylation-dependent endonuclease DpnI (Thermo Fisher Scientific), and bacteria are transformed with the nuclease-resistant nicked plasmid (Fig. 12).

Figure 12

Schematic representation of *in vitro* mutagenesis.

We perform *in vitro* mutagenesis using Phusion™ Site-Directed Mutagenesis Kit (Thermo Fisher™). We amplify plasmid DNA with Phusion™ Hot Start II DNA Polymerase with a couple of primer shown in the Table 4.

hCYFIP2-Mut-editing-For	agatagagctggccagatacattgagaccagtgctc
hCYFIP2-Mut-editing Rev	gagcactggtctcaatgtatctggccagctctatct

Table 4

List of primers used to perform in vitro mutagenesis reactions.

After 15 cycles of two step PCR amplification (98°C 8" – 72°C 4'), the parent template is removed by DpnI digestion (1h30' 37°C). The bacterial transformation was carried out with the same method used to cloning CYFIP2. Plasmids are isolated from the resulting colonies and screened for the desired modification. Finally, the positive clones are sequenced to confirm the desired modification and the absence of additional modifications.

3.8 Protein extraction, quantification and Western Blot

Cells harvested from primary hippocampal cultures were solubilized with modified RIPA (50 mM Tris-HCl, pH 7.4, 150 mM NaCl, 1 mM EDTA, 1% IGEPAL CA630, 0.25% NaDOC, 0.1% SDS, 1% NP-40 and Roche protease inhibitor tablets) and then sonicated. A portion of the lysate was used

for the bicinchoninic acid (BCA) protein concentration assay (Sigma-Aldrich®). Equal amounts of protein were applied to precast SDS polyacrylamide gels (4–12% NuPAGE Bis-Tris gels; Invitrogen) and the proteins were electrophoretically transferred to a nitrocellulose transfer membrane (GE Healthcare, Waukesha, WI, USA) for 2 h. The membranes were blocked for 60 min with 3% non-fat dry milk in TBS-T (Tris-buffered saline with 0.1% Tween-20, Sigma-Aldrich®) and then incubated overnight at 4°C in the blocking solution with the rabbit policlonal anti-CYFIP2 (1:1000; #ab95969 Abcam Cambridge, GB), mouse monoclonal anti-GAPDH (1:10000, #MAB374 Millipore Billerica, MA) primary antibodies. For detection, after 3 washes in TBS-T, the membranes were incubated for 1h at room temperature with IR-Dye secondary antibodies (1:2000 in TBS-T). Signals were detected using an Odyssey infrared imaging system (LI-COR Biosciences) and quantified using Odyssey version 1.1 (LI-COR Biosciences). Data are presented as the ratio of the intensity band of the investigated protein to that of the GAPDH band and are expressed as a percentage of the controls. Each condition was carried out and analysed in 3 independent primary culture dishes.

3.9 Indirect immunofluorescence assay

The cells were fixed with paraformaldehyde (PFA) 4%, washed three times with phosphate buffer saline (PBS) and permeabilized with Triton-X-100 0.3% for 10 min at room temperature (RT). As a saturation compound, the Roche™ blocking solution was used for a 1h incubation; then the primary antibody (rabbit polyclonal anti-CYFIP2, 1:1000, #ab95969, Abcam Cambridge; rabbit anti-HA, 1:150, #H6908, Merck) was incubated for 1h at RT. After three washes with PBS, the cells were incubated with the secondary antibody (Goat anti-Rabbit Alexa Fluor™ 594, #A-11012; Goat anti-Rabbit Alexa Fluor™ 488, #A-11008 Thermo Scientific™) at the adequate dilution for 1h at RT. Again, the cells were washed three times with PBS and then the DAPI staining was performed. The coverslips were then mounted with SlowFade Gold reagent (Thermo Scientific™) and observed under the fluorescent microscope.

3.10 Lentiviral production

Lentivirus were produced according to Filippini and collaborators, (Filippini et al., 2017). The HEK293T cells were plated at low passages (no more than P12-15) 24h before transfection at a density of 9.5×106 in 150mm dish; the medium was changed 2h before transfection. Cells are co-

transfected using calcium-phosphate–DNA coprecipitation method. The plasmids mix used is composed of 3rd-generation transfer plasmids, utilising a hybrid LTR promoter. It is prepared by adding: VSV-G envelope gene in pMD2.G backbone vector 7µg, PACKAGING plasmids pCMV ΔR8.74 II Gen.Pack 16.25µg, pRSV-rev plasmid 6.25µg, Transfer Vector 32µg. The plasmid solution is made up with a final volume of 1225µl with 0.1× TrisEDTA (TE 0.1×)/dH2O (2:1); finally 125µl of 2.5M CaCl2 are added to the suspension; the mixture is maintained 5 min at RT. The precipitate is formed by adding dropwise 1250µl of 2× HBS solution to the mixture. The suspension should be added immediately to the cells following the addition of 2× HBS. The calcium-phosphate plasmid DNA mixture should be allowed to stay on the cells for 14-16h, after which the medium should be replaced with fresh medium. After 24h and 48h from medium replacement, it is necessary to collect the cells supernatant. Then, after the ultracentrifugation of the supernatant at 23000 rpm/2h at 4°C, the viral pellet is resuspended in PBS 1X. After determination of the MOI value (multiplicity of infection, is the number of viral particles that can infect each cell in the tissue culture) of the lentiviral stock solution using HEK293T cell line, we add an amount of MOI 1 of lentiviral particles directly in to the medium

3.11 Generation of SH-SY5Y *CYFIP2-KO* cell line

The CRISPR/Cas system can be implemented in mammalian cells by co-expressing the S. pyogenes Cas9 (SpCas9) nuclease along with the guide RNA.

We use this technology to establish a SH-SY5Y *KO* cell line that is deficient in both *CYFIP2* alleles (*CYFIP2*$^{-/-}$). The SH-SY5Y *CYFIP2 KO* cell line was produced by transfecting WT cells with the Feng Zhang-created plasmid px459 (SpCas9(BB)-2A-Puro (PX459) V2.0) (Ran et al., 2013). This plasmid contains two expression cassettes, a human codon-optimised SpCas9, and the single guide RNA which consists of 76nt of scaffold, required for Cas-binding and 20nt of spacer that identifies the genomic target to be changed. The expression of sgRNA is under the control of U6 promoter, a type III RNA polymerase III promoter commonly used for driving small hairpin RNA (shRNA) expression in vector-based RNAi (Fig. 13). After the vector was BbsI-digested (#ER1011 Thermo Fisher Scientific), two annealed oligos were cloned before the sgRNA scaffold. The oligos are designed based on the target site sequence (20bp) and need to be followed on the 3' end by a 3bp NGG PAM sequence using CRISPOR tool Version 5.01 (http://crispor.tefor.net/) (Concordet & Haeussler, 2018). We have chosen a predicted guide that respects a high rank of MIT specificity

score (Hsu et al., 2013) and a low number of predicted mismatches. After cloning, Stbl3™ Chemically Competent E. coli strain (#C737303 Thermo Scientific™) was transformed to purify PX459-CYFIP2-*KO* DNA plasmid.

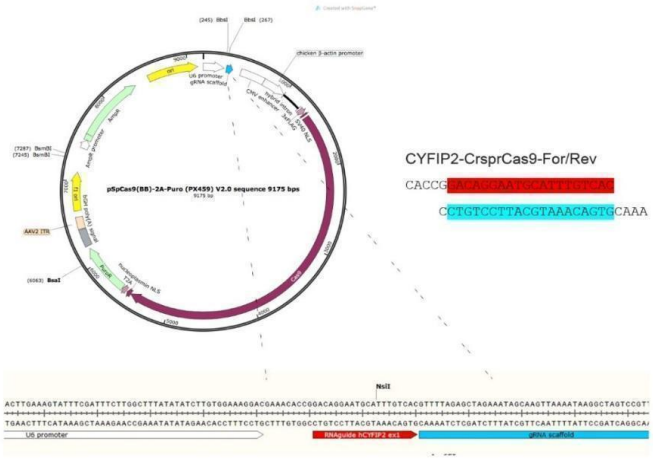

Figure 13

Eukaryotic expression vector SpCas9(BB)-2A-Puro (PX459) V2.0 used to generate CrispR/Cas9 *KO* cell lines.

SH-SY5Y cell line (ATCC™, CRL2266) was transfected with PX459-*CYFIP2-KO* DNA plasmid previously purify using Lipofectamine™ 3000 (#L3000001 Thermo Fisher Scientific), following the manufacturer's protocol.

After determination of the optimal selection antibiotic concentration by performing a kill curve, treating WT SH-SY5Y cells through increasing concentrations of puromycin (#P9620 Sigma-Aldrich®) (Tab. 5), we put transfected cells under antibiotic selection treating them with puromycin at the concentration of 2 ng/µl for 24 hours to exclude untransfected cells.

Puromycin conc. ng/µl	**10.0**	**7.0**	**4.9**	**3.4**	**2.4**	**1.7**	**1.2**	**0.8**	**0.6**	**0.2**	**0.0**
% of live cells	*0*	*0*	*0*	*0*	*0*	*0.4*	*2*	*30*	*70*	*100*	*100*

Tabel 5

Puromycin dose-response kill curve.

After total RNA extraction, the CYFIP2 gene's target region for Cas9 was sequenced to evaluate whether genome editing was present. Following RT reaction, the generated cDNA was PCR amplifying using the intronic primers flanking the target region of genome editing shown in the Table 6. After Sanger sequencing, the resultant electropherogram was assessed using the ICE Analysis tool (Syntego© https://ice.synthego.com/#/).

Int-hDNA-CYFIP2-For	AGATGAAAGGTGGACGCAGCA
Int-hDNA-CYFIP2-Rev	ATGCCTCTGGTGTGAGAAGC

Table 6

List of primers used to amplify the cyfip2 intronic region flanking the exon1, target of genome editing.

3.12 Generation of SH-SY5Y *CYFIP2* K/E *KI* model

In order to generate a stable population of CYFIP2 K and E (SHSY-5Y KI cell lines) we added a MOI 1 of lentiviral particles generating with transgenic vectors pRRLSIN.cPPT.PGK-hCYFIP2-HA.WPRE K or E as previously described, directly in to the medium of SH-SY5Y CYFIP2 *KO* cell lines,

3.13 Generation of hippocampal *CYFIP2* K/E *KI* model

3.13.1 Production of lentiviral vector to downregulate CYFIP2 protein

Vectors to downregulate endogenous CYFIP2 protein were designed starting from TWEEN-Lenti vector (7970bp), that contains the Green Fluorescent Protein (GFP) coding sequence under the control of the hPGK promoter, kindly given by Prof. Leonardo Elia (University of Brescia). Expression of shRNA sequence is under the control of H1 promoter. After the vector was duoble-digested with XbaI and XhoI (#ER0681; #ER0692 Thermo Fisher Scientific), two annealed oligonucleotides carrying the palindromic sequence of shRNA to *Cyfip2* mRNA were cloned. The sequence of shRNA that recognise the 3'UTR sequence of mouse *Cyfip2* transcript in position 3775, were designed using shRNA Optimal Design tool from Kay Lab (https://med.stanford.edu/kaylab). After cloning, Stbl3™ Chemically Competent E. coli strain (#C737303 Thermo Scientific™) was transformed to purify TweenLentiH1-sh3775-Cyfip2 DNA plasmid (Fig. 14).

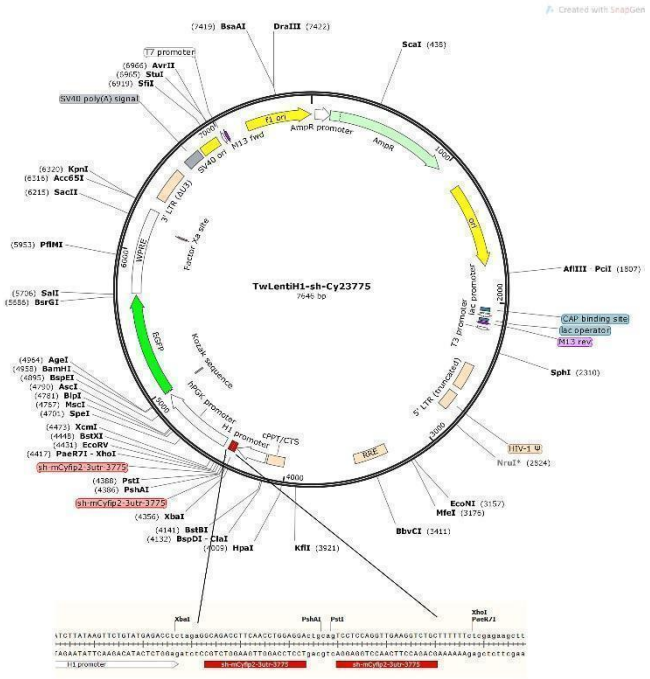

Figure 14

Eukaryotic expression vector TweenLentiH1-sh3775-Cyfip2 used to downregulate CYFIP2 protein in hippocampal culture.

3.13.2 Lentiviral transduction of hippocampal cells

In order to generate a CYFIP2 K/E KI model, hippocampal cultures at DIV1 were transducted adding a mix of lentiviral particles containing TweenLentiH1-sh3775-Cyfip2 to downregulate endogenous CYFIP2 protein and pRRLSIN.cPPT.PGK-hCYFIP2-HA.WPRE K or E to induced the expression of CYFIP2 K or E variants. PFA 4% were used to fix neuronal cultures at DIV4 or DIV17 when they were usedto assess axon development or spine frequency.

3.14 Migration Assay

To set up a “gap closure migration assay” we used SH-SY5Y *CYFIP2-KO* and SH-SY5Y *CYFIP2-KI* K/E cells. Cells were grown in standard condition cell culture media. Cells were transferred into tissue culture treated 12-well plates and grown to 100% confluence. Upon reaching confluence, the cells in the monolayer were starved for 2 h. After starvation, cells were treated in different conditions: Serum starvation environment (SF) and high serum condition (FBS), treating with cell culture media added with 20% FBS (#10270 Gibco™ Thermo Fisher Scientific). Two horizontal

wounds were created manually into each well using a 200 µl pipette tips. Images were captured at intervals of 24, 48 and 36 hours using an inverted light microscope to observe cellular migration (wound closure). Images were individually analysed using image analysis software, and percent wound closure was calculated.

3.15 Confocal microscopy and Imaging Analysis

Fluorescently labelled cells were acquired using an inverted laser scanning confocal microscope LSM900 (Carl Zeiss, Jena, Germany) with a 20x objective at a resolution of 3964 (x/y) pixel. Pictures represent a maximum intensity projection (MIP of 3 Z sections at 1.5 xxx of interval) of 15 consecutive optical sections. Total dendritic length and number of branches were measured using Simple Neurite Tracer from Fiji (Schindelin et al., 2012). For each condition, a number of minimum 15 cells were analysed. The number of spines was measured manually using ImageJ and spine density was calculated by quantifying the number of spines in a 10 µm dendritic segment. For each condition, spines of three secondary dendrites from a minimum of 15 cells were analysed.

4 RESULTS

4.1 Model of *CYFIP2* K/E RNA Editing variants

In 2005, Levanon and colleagues discovered that the *CYFIP2* transcript undergoes RNA editing, an epitranscriptomic modification catalysed by ADAR2 enzyme, which causes the deamination of particular adenosines to inosines. This reaction occurs in the coding sequence of the transcript resulting in K→E substitution at amino acid 320 (Levanon et al., 2005), however its functional meaning is still unknown.

CYFIP2 protein is a component of the Wave Regulatory Complex (WCR), an eteropentameric complex whose crystal structure was revealed in 2010 (PDB: 3P8C) (Z. Chen et al., 2010). Ding and colleagues recently published the highest resolution (~3 Å) structure of the WRC using single-particle cryogenic electron microscopy [36114192]. Two distinct states of the complex were investigated: the constitutively inactive form without Rac1 bounded (PDB: 7USC) (Fig. 15, left) and the active form of complex with Rac1 simultaneously bound to both the A and D sites (PDB: 7USE) (Fig. 15, right).

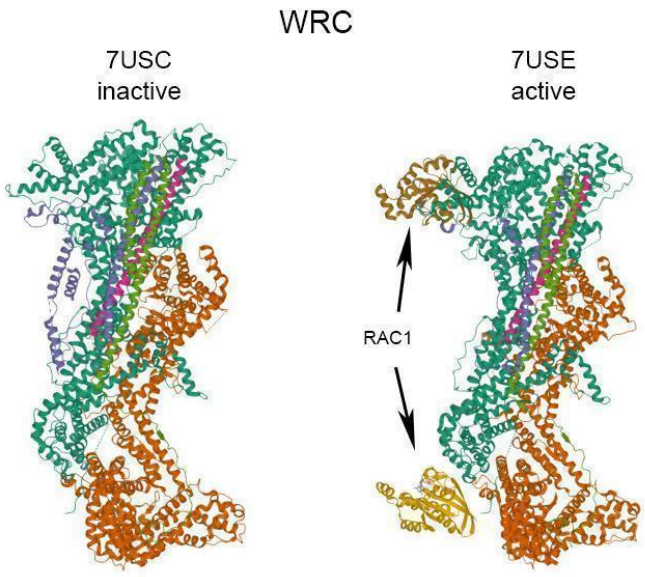

Figure 15

3D reconstruction of experimental structures of WAVE Regulatory Complex (WRC) obtained by Cryo-EM method. Left: constitutively inactive WRC (7USC) (PDB DOI: 10.2210/pdb7USC/pdb). Right: active WRC with Rac1 bound on both A and D site (7USE) (DB DOI: 10.2210/pdb7USE/pdb).Modify from (Ding et al., 2022).

Both WRCs derived from crystal structure (3P8C (Z. Chen et al., 2010)) or cryo-EM (7USC, 7USE (Ding et al., 2022)) represent a pentameric complex composed of CYFIP1, NCKAP1, WAVE1, Abi2, and HSPC300 proteins. Due to the high degree of similarity between the CYFIP1 and CYFIP2 proteins (95%), we built a homology model of the complex using CYFIP2 instead of CYFIP1. (Biembengut et al., 2022). We took advantage of Dynamut2 tool (https://biosig.lab.uq.edu.au/dynamut/ (Rodrigues et al., 2021)) to analyse and predict protein stability and flexibility changes after K→E substitution following the RNA editing process. Structural changes in WRC are visible in Figure 16.

The obtained results indicate that the edited variant (E) might lead to a destabilisation of the complex with a predicted Stability Change (ΔΔGStability) of -0.3 Kcal/mol when we analysed the inactive form of WRC (7USC). The effect of K/E editing on WRC stability seemed to be different in fully active WRC (7USE), with an increase in $\Delta\Delta G^{Stability}$ of +0.04 Kcal/mol, as shown in Table 7.

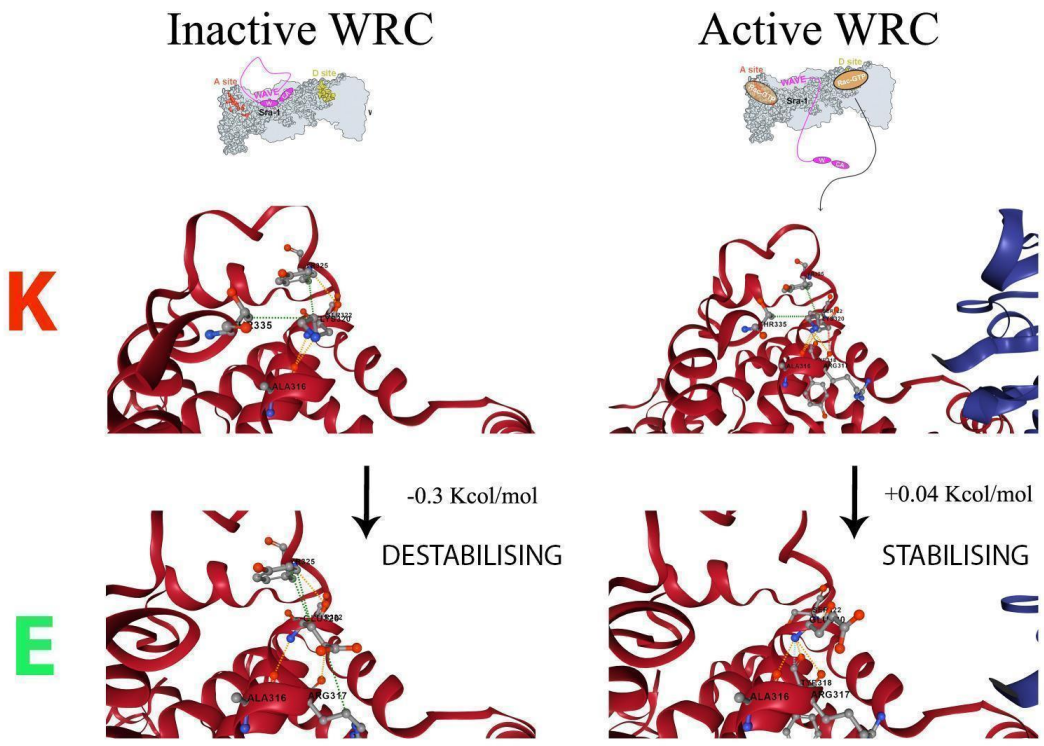

Figure 16

Normal Mode Analysis of 3D structures obtained by Dynamut tool. Conformational changes of inactive (left 7USC) or active (right 7USE) WRC after K/E substitution.

PDB	7USC	7USE
WRC state	Inactive	Fully active
ΔΔGStability *Kcal/mol*	- 0.3	+ 0.04
Predicted effect	*DESTABILISING*	*STABILISING*

Table 7

Prediction of protein stability change upon K/E substitution using Mutation Effect Prediction by Dynamut tool.

These results suggest that the RNA editing of *CYFIP2* might give different characteristics to the active or inactive WRC. In particular, the prediction of the decrease of the complex stability after insertion of glutamate (E) instead of lysine (K) in the inactive form of WRC (7USC), leads to hypothesise that editing regulation can have a greater impact in the inactive WRC form respect to the active complex (7USE) in which the stability is substantially unchanged.

4.2 *CYFIP2* K/E 320 RNA Editing modulation

Site-selective adenosine to inosine (A-to-I) RNA-editing is an essential post-transcriptional mechanism for expanding the proteomic repertoire (Bass, 2002). *CYFIP2* RNA editing was discovered by Riedmann and colleagues to be highly prevalent in neural tissue (Riedmann et al., 2008). RNA interference studies revealed that ADAR2 is the primary editing enzyme involved in this process (Riedmann et al., 2008). To get new insights in the functional role of *CYFIP2* RNA editing in neuronal development, we have examined its level in mouse primary hippocampal neurons cultures at different Day *In Vitro* (DIV) as a model of neuronal maturation. The analysis has been done using Sanger sequencing technique. Our findings demonstrated that the RNA editing reaction increased during *in vitro* neural development (DIV4: 14.5%; DIV7: 23.5% DIV14: 44%; DIV21: 59.5%) (Fig. 17, left), indicating that the level of editing at the K/E site is tightly regulated.

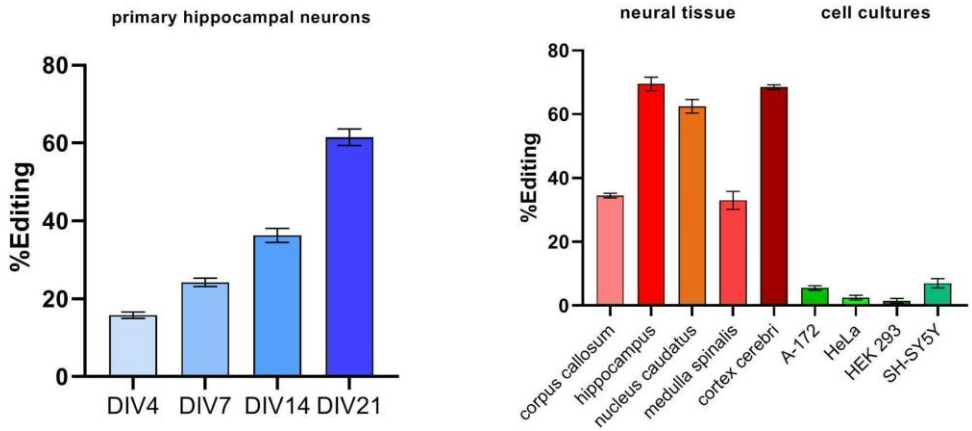

Figure 17

Analysis of editing levels of the CYFIP2 K/E site during *in vitro* primary hippocampall neuron maturation (left) and in several human brain regions and cell lines (right).

Furthermore, RNA editing levels in different human post-mortem brain regions and non-neural cell line samples have been examined (Fig. 17, right). The editing percentage obtained from neural tissue samples are: Corpus Callosum (CC) 35%; Hippocampus (Hi) 71%; Caudate (Nc) 61%; Spinal Cord (Sc) 31% and Cerebral Cortex (Cx) 68%. Editing percentage obtained from non-neural cell lines are respectively: glioblastoma (A-172) 6%; Human cervix epitheloid carcinoma (HeLa) 2%; human embryonic kidney (HEK293) 1%; human neuroblastoma (SH-SY5Y) 6%.

To have an overview of RNA editing per RNAseq experiment, we used the REDI portal database (http://srv00.recas.ba.infn.it/atlas/), one of the most up-to-date atlas of RNA editing, based on 9642 human RNAseq samples from 549 individuals (31 tissues and 54 body sites). As shown in Figure 18, the RNA editing levels obtained from human *CYFIP2* transcripts result higher in neuronal tissues, thus confirming our and previous evidence of being a neuron-specific process.

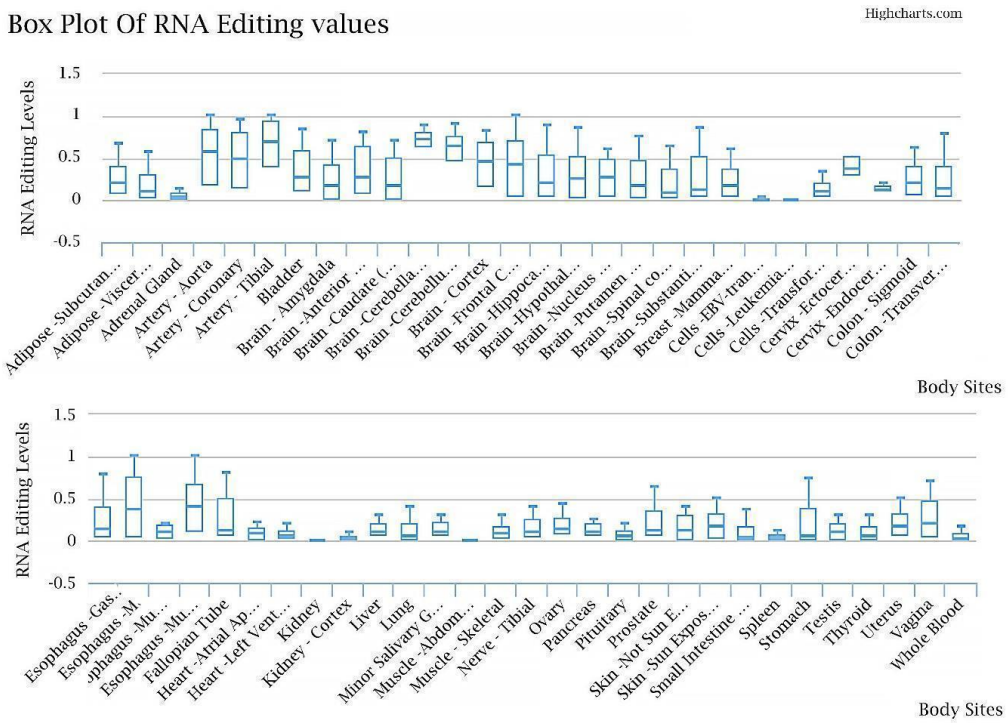

Figure18

Editing levels of human CYFIP2 transcripts obtained from RNAseq experiment (REDI portal database).

We used mouse primary neuronal cultures as a model to determine whether the CYFIP2 editing reaction can be modulated by physiological processes. Hippocampal neurons were exposed to a non-toxic dose of glutamate (10µM) for 24 hours to mimic glutamatergic activation. Cells were collected immediately after treatment. We discovered that glutamate treatment led to a decrease of *CYFIP2* editing levels (Student t-test −56.4%; $P < 0.001$) (Fig. 19).

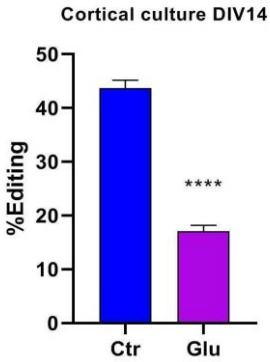

Figure 19

Analysis of editing levels of the CYFIP2 K/E site in hippocampal neurons treated for 24h with 10µM glutamate to mimic neuronal activity (Student t test: **** $p<0.0001$).

Our findings demonstrate that the *CYFIP2* RNA editing process is specifically controlled in various brain regions and is only active in the central nervous system. A proper *CYFIP2* editing regulation is important during neuronal development and for neuronal function leading to the hypothesis that its dysregulation might be involved in neurodevelopmental disorders.

4.3 Analysis of CYFIP2 K/E amino acid conservation during evolution

To further investigate the importance of K/E RNA editing modification, we analysed the conservation rate of CYFIP2 protein in different species. We studied genes similar to CYFIP2 using NCBI Orthologs database (https://www.ncbi.nlm.nih.gov/gene/26999/ortholog/?term=CYFIP2). A number of 438 genes for jawed vertebrates (Gnathostomata) have been processed by aligning their protein sequences using Constraint-based Multiple Alignment Tool COBALT (https://www.ncbi.nlm.nih.gov/tools/cobalt/cobalt.cgi). CYFIP2 protein presents a high rate of conservation between the different species. At the position of the amino acid subjected to editing regulation, Lysine (K) is present in the 68.5% of the protein sequences analysed (n=300). Interestingly, in 29,9% is present Glutamic acid (E) (n=131). 1,6% (n=7) is represented by a third amino acid different between K and E.

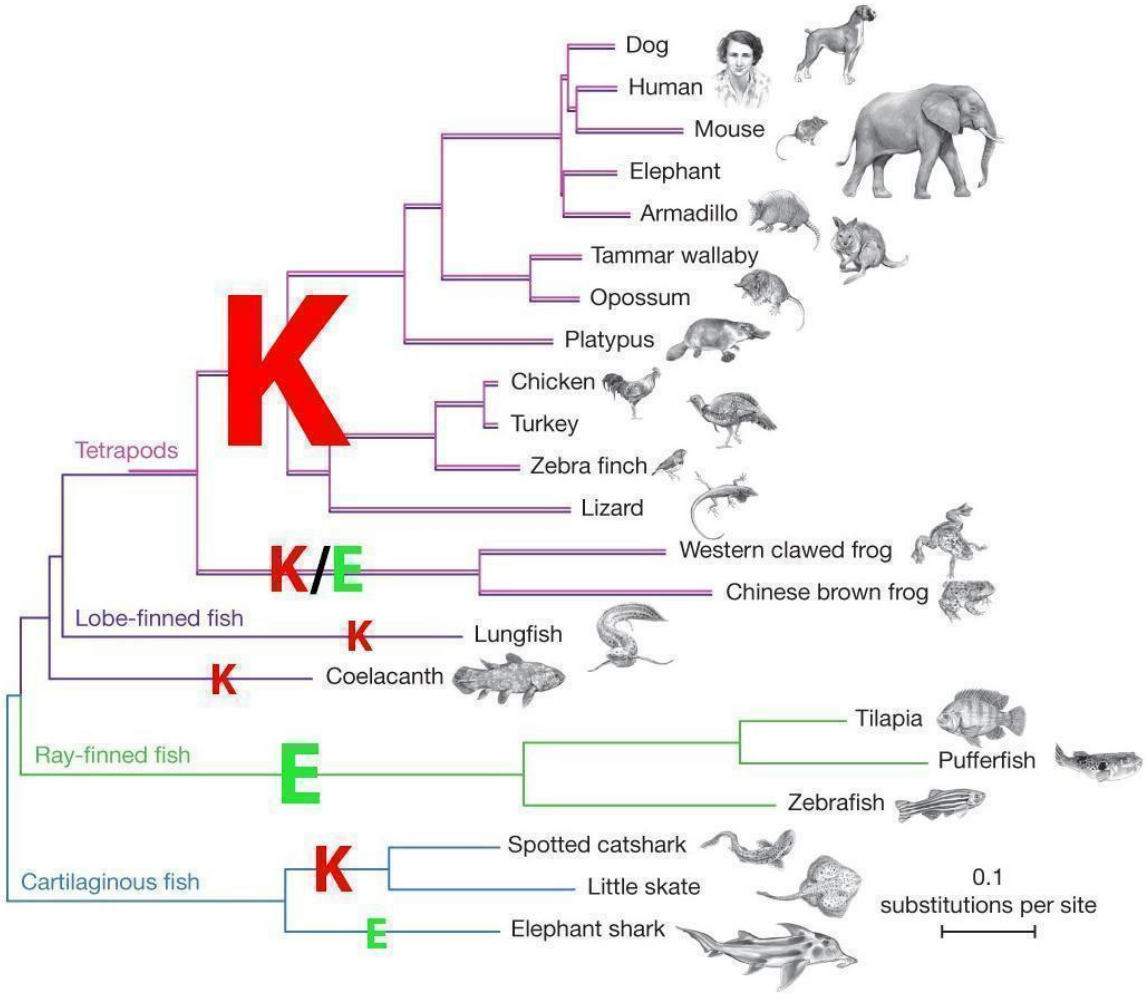

Figure 20

Jawed vertebrate phylogenetic trees show the conservation of K/E amino acid in the site of RNA editing regulation of CYFIP2 orthologous genes in different species [modified from 23598338].

Observing at the DNA level, the conservation of the amino acid residue present at the position subject to RNA editing, it appears evident how both Lysine (K) and Glutamate (E) are present during evolution. From amphibians, where some species get the amino acid K and others contains E, to the later classes of vertebrates including reptiles, birds and mammals, all have the amino acid K. When looking backward in evolution, the E is present in every superclass of bony fishes (Osteichthyes) but in their forebears, the cartilaginous fishes, we find the K afterwards—with the exception of the Elephant sharks (Callorhinchus milii), in which we also find the K again.

These findings suggest that both amino acids at this specific position of the CYFIP2 protein are tolerated and possibly contribute to the protein's physiology.

4.4 Generation of SH-SY5Y *CYFIP2 KO* cell line using CRISPR/Cas9-mediated genomic deletion

In order to gain insight into the function of *CYFIP2* K/E RNA editing physiological process, we decided to use a neuroblastoma SH-SY5Y cell line as an *in vitro* model, due to the ability of these cells to migrate, proliferate, and develop into cells with a neuronal phenotype. The use of SH-SY5Y allows us to examine the function of CYFIP2 in moving and mitotic cells as well as to simulate their maturation into a neuronal phenotype.

We have established a SH-SY5Y *KO* cell line that is deficient in both *CYFIP2* alleles ($CYFIP2^{-/-}$) using the recently developed CRISPR-Cas9 technology (Cong et al., 2013). Furthermore, through the transduction of lentiviral particles carrying the whole CDS of human *CYFIP2* K/E forms, *KO* cell line was used to create *CYFIP2* Edited (K) and Unedited (E) *Knock-In* cell lines.

The SH-SY5Y *CYFIP2 KO* cell line was produced by transfecting WT cells with the Feng Zhang-created plasmid px459 (SpCas9(BB)-2A-Puro (PX459) V2.0) (Ran et al., 2013), in which the RNA guide sequence that recognizes the first exon of the endogenous *CYFIP2* gene was previously cloned. This plasmid carries the expression of Cas9 from *S. pyogenes* with 2A-Puro and *Single Guide RNA* (V2.0) which consists of 76 nt of scaffold, required for Cas-binding and 20 nt of spacer that identifies the genomic target to be changed. The expression of sgRNA is under the control of U6 promoter, a type III RNA polymerase III promoter commonly used for driving small hairpin RNA (shRNA) expression in vector-based RNAi. Once produced in the cell, sgRNA molecules drive Cas9 enzymes to his target sequence located on the first exon of *CYFIP2* gene and carry out a double-strand break (DSB) within the target DNA (Fig. 20). The resulting DSB is then repaired by one of two general repair pathways: the efficient but error-prone non-homologous end-joining (NHEJ) pathway, or the less efficient but high-fidelity homology directed repair (HDR) pathway. The NHEJ repair pathway is the most active repair mechanism, and it frequently causes small nucleotide insertions or deletions (indels) at the DSB site. The randomness of NHEJ-mediated DSB repair has important practical implications, because a population of cells expressing Cas9 and a gRNA will result in a diverse array of mutations. In most cases, NHEJ gives rise to small indels in the target DNA that result in amino acid deletions, insertions, or frameshift mutations leading to premature stop codons within the open reading frame (ORF) of the targeted gene (Fig. 21).

The design of gRNA, created using CRISPOR tool (Concordet & Haeussler, 2018), was complementary to the exon 1 of the target site sequence (Fig. 20). Plasmid DNA carrying the expression of gRNA, Cas9 protein and puromycin resistance was transfected in SH-SY5Y cell line.

After antibiotic selection, total RNA of cells was purified, retrotranscribed and amplified using the intronic primers flanking the target region of genome editing. and sequenced, to evaluate whether genome editing was present.

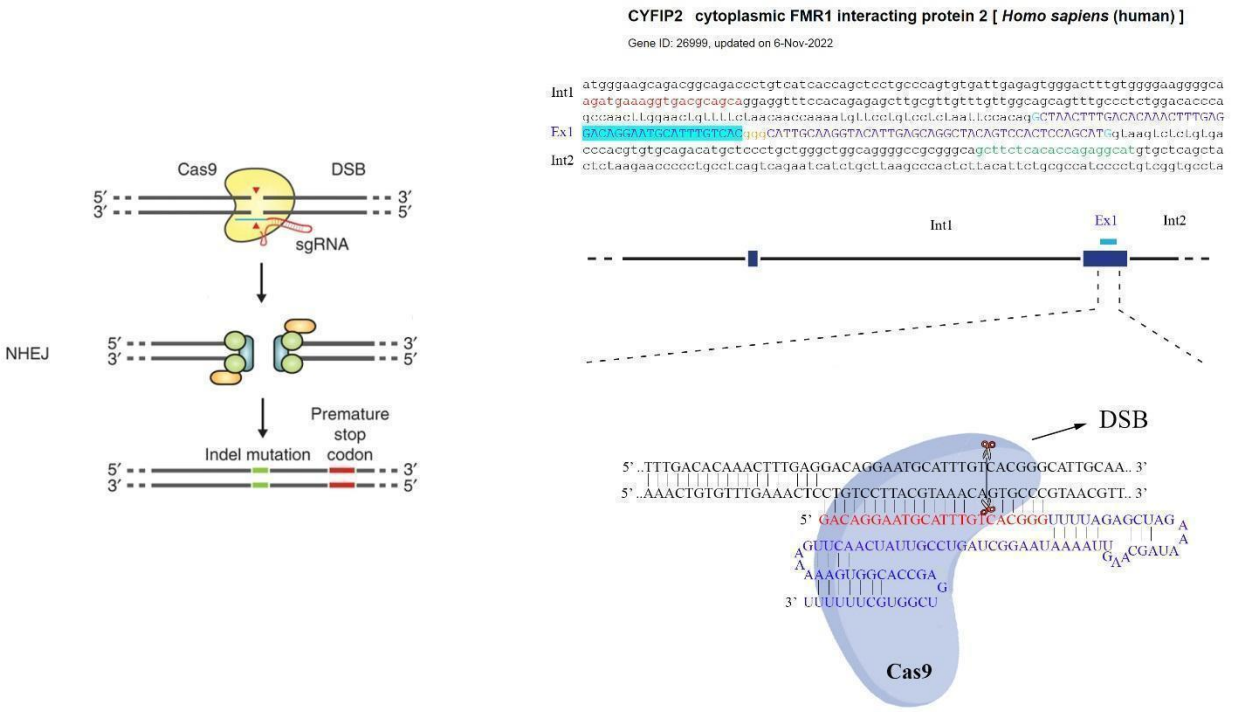

Figure 21

Schematic representation of CRISPR/Cas system. The ends of a DSB are processed and rejoined by endogenous DNA repair machinery in the error-prone NHEJ pathway, which can cause random indel mutations at the junction location. Gene knockout can come from indel mutations that cause frameshifts and the development of an early stop codon in a gene's coding region (Left) (modified from (Ran et al., 2013). In cyan, sgRNA target sequence followed by a GGG PAM motif, placed in the first exon of human CYFIP2 gene (Top, right). Representation of the DSB operated by Cas9 protein on the CYFIP2 gene (black sequence), after sgRNA (red sequence) recognition and binding (Right, bottom).

After Sanger sequencing, the resultant electropherogram was assessed using the ICE Analysis tool (Syntego© https://ice.synthego.com/#/), a software that offers fast and reliable analysis of CRISPR editing data. After analysis, we obtained 96% of indel mutations with the same percentage of *KO* score (Fig. 22, top). The results showed a large prevalence of the same mutation; in particular, 73% of molecules presented an insertion of one Thymine (+1). The other most represented mutations are all deletions: -1 (11%); -2 (6%); -7 (2%) (Fig. 22, bottom).

Figure 22

Output obtained from Syntego© ICE Analysis tool. Comparison of electropherograms of the sgRNA recognition sequence (black underlined), obtained from sequencing of edited and WT samples (top). Alignment of different sequences present in the edited sample with relative contribution in percentage (bottom).

These findings demonstrate that the Crispr/CAS9 experiment developed is highly efficient. If the detected mutations are translated into proteins, they cause premature stop codons and frame-shift. The total absence of WT sequences and the presence only of frameshift mutations, indicate that we have generated a homozygous *CYFIP2 KO* cell line.

A western blot analysis was performed to confirm the absence of the CYFIP2 protein in the cell line as shown in Figure 23.

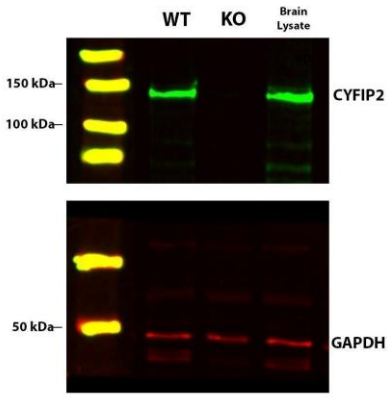

Figure 23

IR acquisition of WB obtained from cellular lysate derived from WT SHSY-5Y cell line (WT), cellular lysate from SHSY-5Y cell line after CRISPR/Cas9 and puromycin selection (*KO*) and mouse brain lysate as a positive control. Endogenous CYFIP2 proteins are detected using rabbit-α-CYFIP2 antibody.

4.5 Phenotypic alteration of SH-SY5Y *CYFIP2 Knock-Out* cell line

Plasma cellular blebbing is a cellular process induced by a combination of events that involve local disruption of membrane–actin cortex interactions, leading to rapid protrusion of the plasma membrane, associated with the appearance of cell blebs. These structures are characterised by a bulge of the plasma membrane that forms a large, approximately spherical distortion of the cell surface (Charras et al., 2005). There are several examples in the literature in which interference with lamellipodia formation promotes plasma membrane blebbing. Inhibition of lamellipodia through blocking WRC or Arp2/3 complex functionality promotes formation of plasma membrane blebs in various cell types in distinct organisms (Suraneni et al., 2012).

SH-SY5Y-WT cells have non-polarized cell bodies characterised by a neuroblast-like phenotype with a few shortened processes (Fig. 24 top, left) while SH-SY5Y-*CYFIP2 KO* cells exhibit a striking morphological change with the formation of cell blebs on the plasma membrane (Fig. 24 top, right).

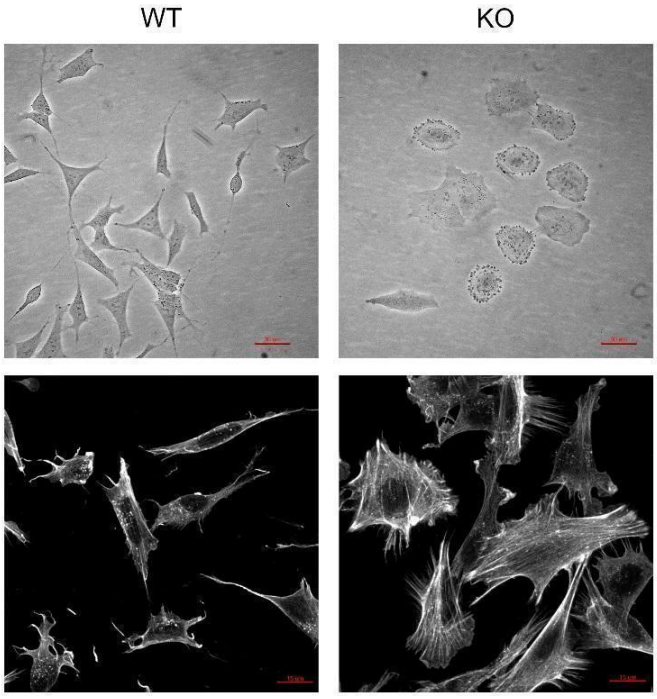

Figure 24

Morphological alteration of SH-SY5Y cell line after *CYFIP2* gene knocking down. Phase contrast microscopy images of SH-SY5Y wt (top, left) and SH-SY5Y *KO* (top, right) (Optech Biostar IB 20X scale bar: 30 μm). Phalloidin staining of SH-SY5Y cell line wt (bottom, left) and *CYFIP2-KO* (bottom, right) (Zeiss© LSM880 40X scale bar: 15 μm).

LSM confocal microscopy was used to evaluate the F-Actin filaments organisation, after fixation and staining with Alexa Fluor™ 647 Phalloidin conjugated probe. As can be observed at the bottom of the Figure 24, *KO* cells showed a completely different actin filaments organisation compared to WT cells.

4.6 Phenotypic rescue of SH-SY5Y *CYFIP2* K/E *Knock-In* cell line

We choose to create a stable SH-SY5Y *CYFIP2 KI* cell line to determine if the F-Actin dependent morphological changes observed in *CYFIP2 KO* cells are brought on specifically by *CYFIP2* gene knocking down.

We produced lentiviral particles containing the *CYFIP2* K and E variants, cloning in a backbone from 3rd generation lentiviral vector pRRLSIN.cPPT.PGK-GFP.WPRE, the human CDS of *CYFIP2* gene (NM_001037333.3). The cells were transduced with high MOI in order to produce stable populations of SH-SY5Y *CYFIP2* KI cells. We performed a WB analysis to determine whether a transgene was expressed in transduced cells (Fig. 25).

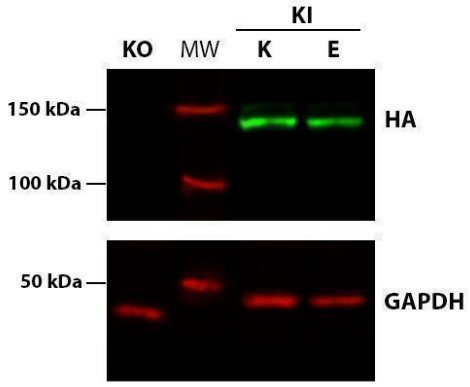

Figure 25

IR acquisition of WB obtained from cellular lysate derived from *KO* SHSY-5Y cell line (*KO*), and KI SHSY-5Y K or E samples. Exogenous CYFIP2 proteins are detected using rabbit-α-HA antibody.

The presence and localisation of the transgene was also examined using IF experiments after one week of standard condition cell growth. To study cytoskeletal organisation, F-Actin filaments were stained with an Alexa Fluor™ 647 Phalloidin tagged probe.

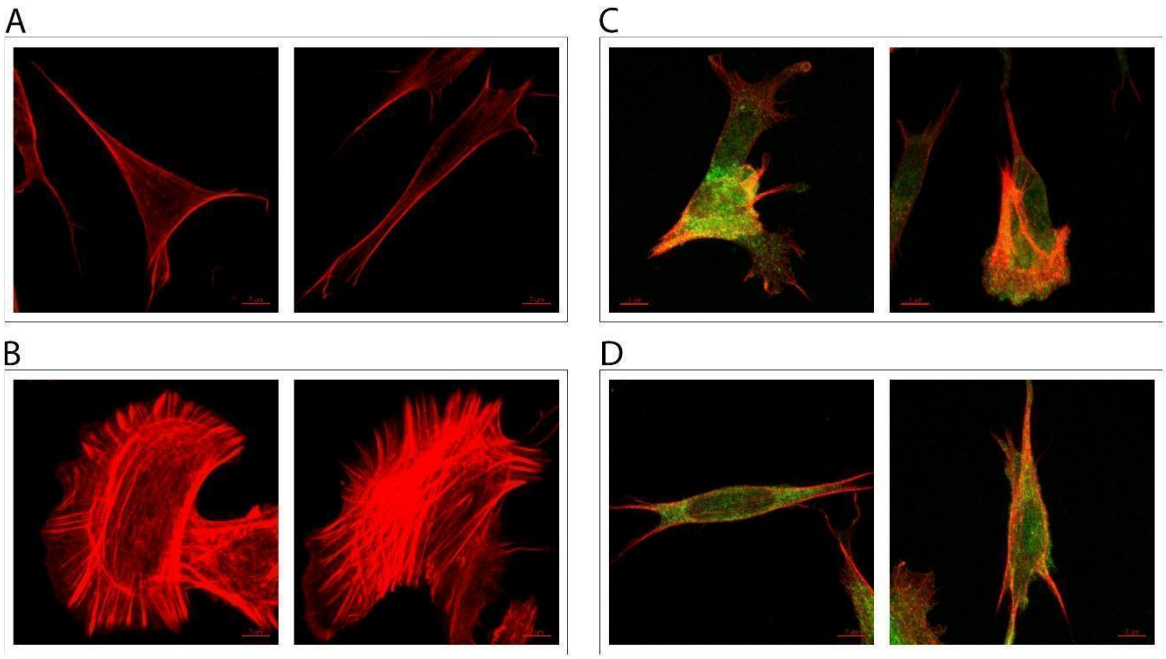

Figure 26

SH-SY5Y WT (A) and CYFIP2 *KO* (B) and overexpressing HA- CYFIP2-320K (C) and HA-CYFIP-320E variants (D). Actin filaments are stained by phalloidin (red) while exogenous CYFIP2 is stained with HA antibodies (green).

As reported in Figure 26 B, after *CYFIP2* gene knockdown, SH-SY5Y cells lost their characteristic neuroblast-like phenotype. However, the morphological phenotype can be reverted when both CYFIP2 K and E variants are overexpressed (Fig. 26 C,D). This finding supports the evidence of the central role of CYFIP2 protein in the F-Actin dependent cytoskeleton organisation.

4.7 Migration Assay

Since the actin polymerization process is closely related to cell migration, we investigate if CYFIP2 K/E variants can have different impact on this process using a "gap closure migration assay".

Cells were grown in standard condition cell culture media upon reaching confluence. Then, the cells in the monolayer were growth in serum deprivation condition for 2 h. The cells are then treated in different conditions: Serum deprivation environment (SF) and high serum condition (FBS), treating with cell culture media additioned with 20% FBS to model inactive/active WRC respectively. Images were captured at intervals of 24, 48 and 36 hours using an inverted light microscope to

observe cellular migration (wound closure). Images were individually processed using ImageJ analysis software, measuring the area of gap closure after each time point and percent of wound closure was calculated (Fig. 27, top). One-way ANOVA showed statistically significant differences among different groups of both experimental tested conditions. In particular, when the cell line growth in serum free conditions (SF), both *KI* cell lines (K and E) showed an increase in migration ability compared to *KO*. The cells overexpressing the edited CYFIP2 form (E), show a stronger migration ability respect the cells overexpressing the unedited CYFIP2 form (K) (p=0.0003 at 24h, p=0.0010 at 36h and p=0.0017 at 48h). The experimental condition in the presence of FBS 20% (FBS) showed a similar results, but the difference between cells overexpressing K or E CYFIP2 variants are less marked (p<0,0001 in each of three times analysed) (Fig. 27, bottom).

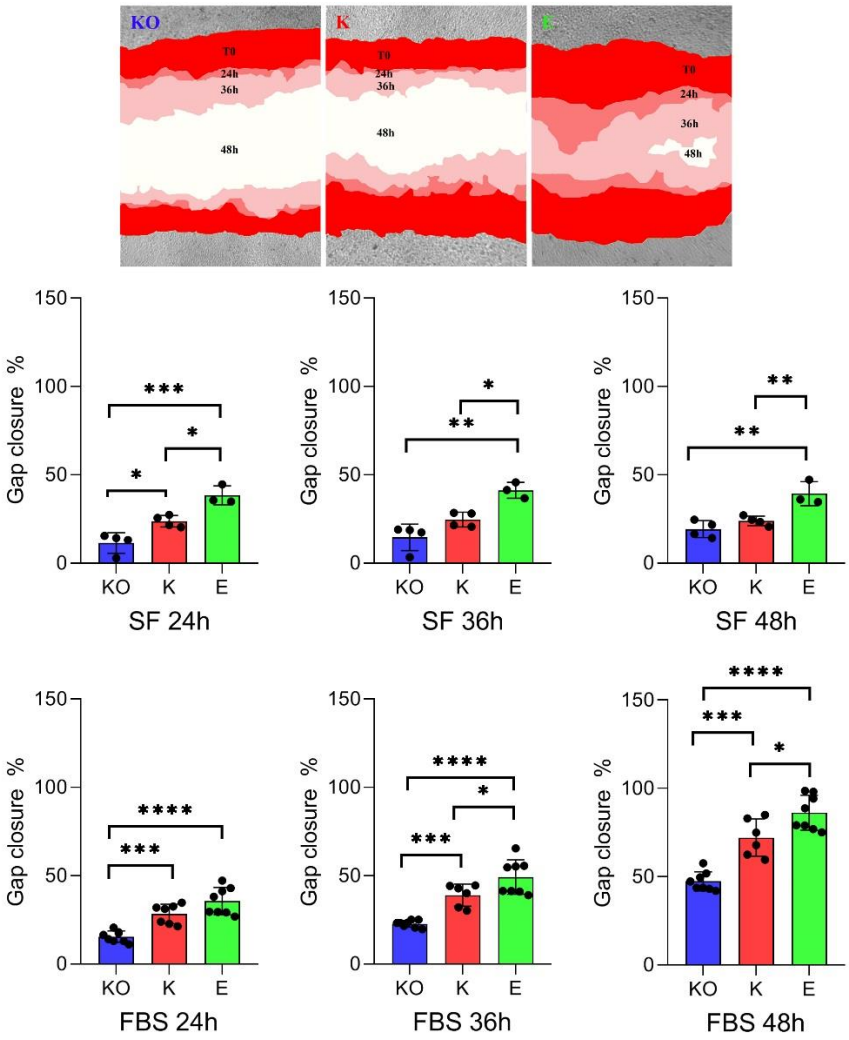

Figure 27

Wound healing assay analysis of SH-SY5Y CYFIP2-*KO*, K or E variants at different time points. The assay has been performed in serum free conditions (SF) and after serum stimulation (FBS) (Tukey's multiple comparisons test: *<0.05 ** <0.01 ***<0.001 ****<0.0001).

Our results showed differences of the edited and unedited CYFIP2 proteins in regulating cellular migration. In particular, the edited variant (CYFIP2-E) presents a stronger capability to migrate and to invade the experimental wound both in starvation conditions and under growth factors stimulation. These data indicate that the editing reaction might be involved in the acting dynamic underlining cellular migration and proliferation.

4.8 Neurite development during SH-SY5Y differentiation

Since CYFIP2 protein is mainly expressed in neurons (Zhang et al., 2019) and K/E RNA editing reaction is active only in the central nervous system (Levanon et al., 2005), we investigated the role of CYFIP2 K/E variants on neuronal development. For this purpose, we used a well-established model of neuronal differentiation based on the application on SH-SY5Y cells of a two-step retinoic acid (RA) and brain-derived neurotrophic factor (BDNF) treatment (Hromadkova et al., 2020)bdnf (Fig. 28, top) to monitor the induction of undifferentiated SH-SY5Y into neuron-like cells with distinctly polarised axon-dendritic morphology. After RA administration and subsequent FBS starvation, it is feasible to see a brief decrease in cell density in both *KI* cell types. The remaining cells have spindle-like morphologies with polarised appearances, with sporadic shafts and projections extending from soma, usually one per cell. When these cultures were exposed to BDNF, cellular processes expanded quickly and dramatically and took on identifiable neurite-like characteristics. In contrast, after the differentiation protocol, *CYFIP2 KO* cells display a characteristic fibroblast-like morphology with a non-polarized appearance and large soma (Fig. 28, bottom).

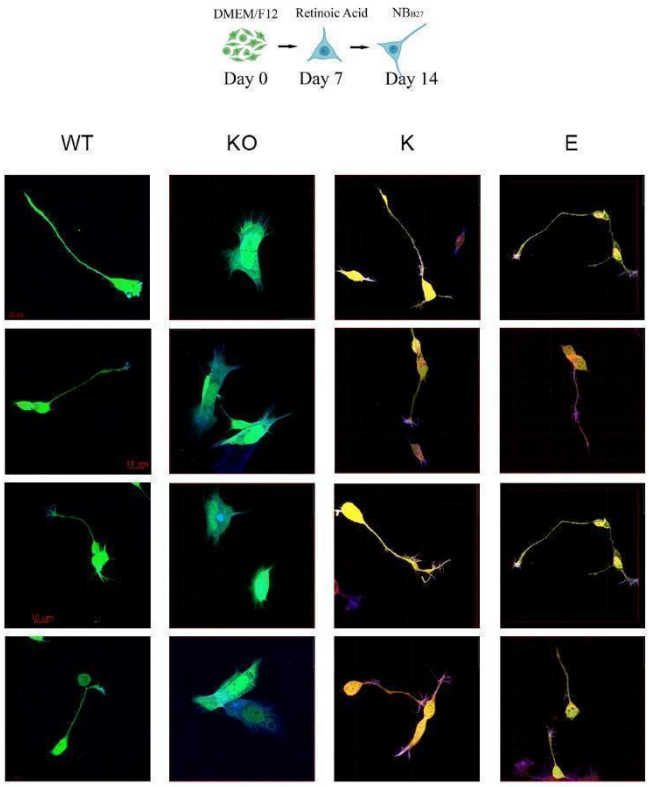

Figure 28

After differentiation, CYFIP2 *KO* cells do not develop a neural-like morphology visible in WT population. Neuron-like cells with distinctly polarized neurite, are visible after CYFIP2 gene KI (K, E). Phalloidin Alexa fluor 647 in blue; GFP in green; CYFIP2-HA Alexa fluor 594 in red. Images are acquired through Zeiss LSM880 confocal microscope with 40x magnification.

The analysis and comparison of principal neurite length of cells using ImageJ's framework Simple Neurite Tracer (SNT), clearly demonstrates that *KO* cells have lost their ability to produce a characteristic neurite-like morphology after differentiation. The length of neurites were: WT mean length = 56.0 ± 3.69, n = 243; *KO* mean length = 15.89+/- 1.17, n = 173; K mean length = 53.34+/- 2.89, n = 192; E mean length = 60.04+/- 4.21, n = 191. One-way ANOVA showed statistically significant differences among the group ($p<0.0001$). Tukey's multiple comparisons test showed a dramatic decrease after Knocking down the *CYFIP2* gene expression. Furthermore, the ability of neurite development is completely restored in both *CYFIP2 KI* cell populations (K/E). (WT vs *KO* Mean diff. 40.14, $p <0.0001$; *KO* vs K Mean diff. -37.45, $p <0.0001$, *KO* vs E Mean diff. -44.15, $p <0,0001$). However, no differences could be detected between *KI* K and E cell populations (K vs E Mean diff. -6.70, $p = 0.51$), indicating that *CYFIP2* is important for neuronal differentiation but the two isoforms might have a similar function regarding this process in SH-SY5Y model (Fig. 29).

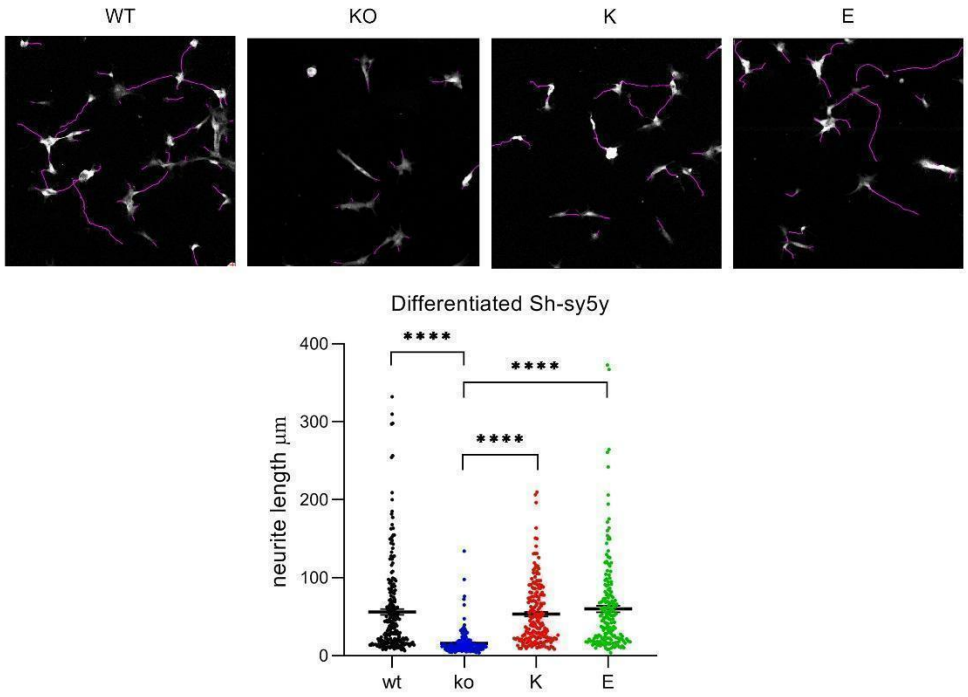

Figure 29

Neurite tracing of different populations of SHSY-5Y of cells by Simple Neurite Tracing (Top). One-way ANOVA followed by Tukey's multiple comparisons test analysis showed that *CYFIP2 KO* cells do not develop a neural-like morphology visible in WT population. The length of neurite was different between *KO* cells and other populations of cells (B). No differences could be detected between K and E cell populations (N= 243 (WT), 173 (*KO*), 192 (K), 191 (E); Tukey's multiple comparisons test: ****<0.0001). (Bottom).

4.9 Study of axon development of hippocampal primary neurons

Since we did not observed a clear difference between CYFIP2 K/E variants in neural maturation process using SH-SY5Y RA-BDNF as a model, we took advantage of primary neuronal culture model (Orlandi et al., 2011) to try to understand the effect of CYFIP2 variants on neuronal maturation.

In order to down-regulate the expression of the endogenous CYFIP2 protein, we transduce primary hippocampal neuronal cultures at DIV1 with lentiviral particles containing a shRNA targeting the 3'UTR of *Cyfip2* gene. To test the efficiency of gene silencing, CYFIP2 expression analysis by western Blot was performed. As can be observed in Figure 30A, 48 after transduction the levels of endogenous CYFIP2 protein is reduced by 70.2%. Silenced cells were co-transduced with lentiviral particles carrying the expression of the CDS of human *CYFIP2* K or E exogenous variants, to study

the impact of edited or unedited CYFIP2 variants in a model of *in vitro* neural maturation. Western blot analysis was performed to check the presence of exogenous CYFIP2 variants eighteen days after lentiviral transduction (Fig. 30 B), by western blot against HA epitope.

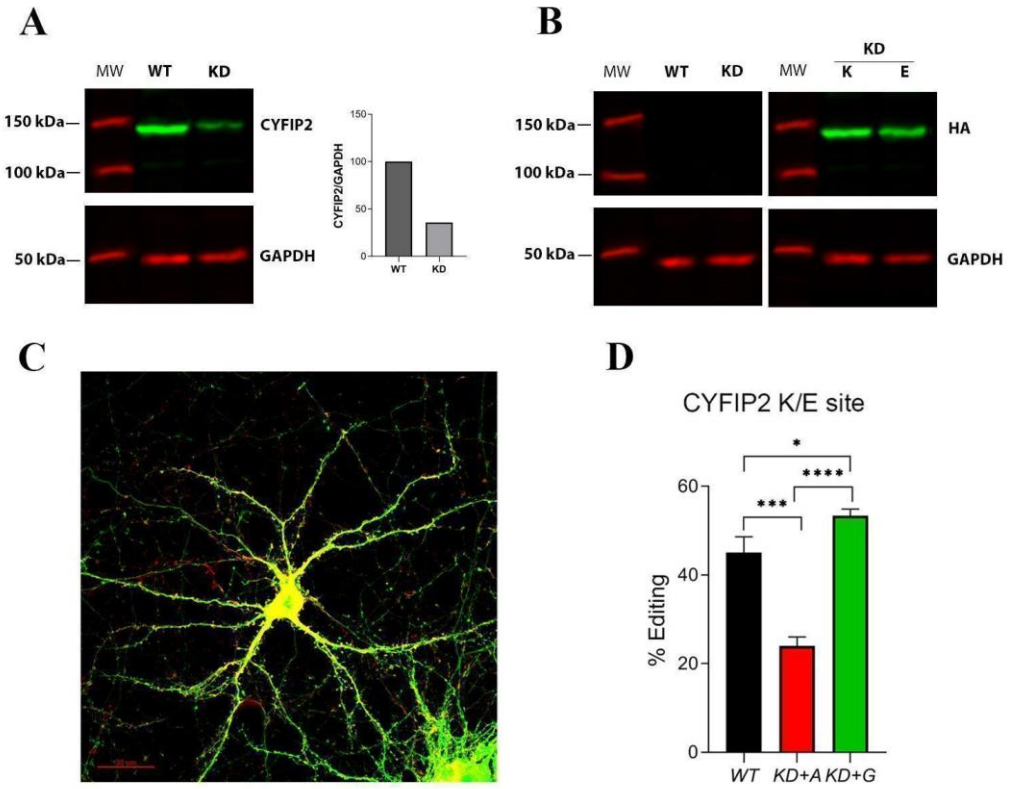

Figure 30

IR acquisition of WB obtained from cellular lysate derived from WT Hippocampal culture (WT) and after 48 from Lentiviral transduction of shRNA targeting the 3'UTR of *Cyfip2* gene (*KD*). Endogenous CYFIP2 protein is detected with rabbit-α-CYFIP2 antibody. In the graph is shown the CYFIP2 downregulation percentage (A). Cellular lysate of *KD* hippocampal cells growth for 18 DIV after lentiviral transduction with CDS of human CYFIP2 K or E variants. Exogenous CYFIP2 proteins are detected using rabbit-α-HA antibody (B). Hippocampal cell at DIV18 captured by confocal microscopy. The GFP protein, which represents a marker for CYFIP2 down-regulation, is detected in green. Exogenous CYFIP2 is visible in red (rabbit-α-HA antibody - goat-α-rabbit Alexa Fluor 594) (C). CYFIP2 K/E Editing levels calculated from total RNA samples obtained from *wild-type* hippocampal cell (WT) or CYFIP2 *knock-down* hippocampal cell transduced with two editing variants (*KD*+A; *KD*+G) (D) (Tukey's multiple comparisons test: *<0.05 ** <0.01 ***<0.001 ****<0.0001).

Since the vector carrying the shRNA also contains the sequence coding for green fluorescent protein (GFP), we can evaluate the extent of transduction by fluorescence microscopy technique (Fig. 30C). To validate our model of *CYFIP2* RNA editing modulation, we decided to evaluate the real amount of *CYFIP2* editing variant expressed in our experimental groups. We extracted total RNA from cells that had been cultured for 14 days. The cDNA resulting from retrotranscription reaction, was then amplified through PCR and *CYFIP2* editing levels were subsequently analysed by Sanger sequencing. As can be seen in Figure 30D, the hippocampal neurons silenced in endogenous CYFIP2

protein that overexpress CYFIP2 K or E variant (*KD*+A) exhibit respectively 24 and 53 % of RNA editing percentage.

Christine Holt's group elegantly explained how CYFIP2 is involved in the growth and sorting of retinal ganglion cells axons, using *in vivo* and *in vitro* models [29518358]. For this reason, we initially focused on the early stages of neuronal maturation analysing neuronal axon length during the first days of *in vitro* neuronal growth.

In hippocampal neurons at DIV1, we co-transduced lentiviral particles expressing CYFIP2 K or E variants with lentivirus expressing shRNA to downregulate endogenous CYFIP2 protein, in order to assess the impact of RNA editing alteration, excluding the effect of endogenous protein. The cells are fixed after 72 hours and images, made up of an array of 20x20 frames, are captured using a 40X magnification by Zeiss© LSM 900 confocal microscope. Using Simple Neurite Tracer (SNT) (Arshadi et al., 2021), an ImageJ's framework for analyses of neuronal morphology, we plotted a minimum of 44 neural axons for each population of cells to obtain the number of branches, total axon length and complexity index (a function of neurite attachment points and ending points) (Fig. 31, top). We found a statistically significant difference among WT, *CYFIP2 KO* and neurons carrying K and E variants in each of the three parameters considered (One-way Anova Test - N° of branches; Path length [sum] μm; Complexity Index log2: $p<0.0001$). Tukey's multiple comparisons test showed a reduction in the N° of branches and Path length after Knocking down the *CYFIP2* gene. Furthermore, the ability to produce axons with proper complexity is completely restored when *KD* neurons were grown overexpressing the E variant of the CYFIP2 gene, but not with the K variant. The complexity of the axons in neurons carrying CYFIP2 E variant is statistically significantly higher even in comparison of WT neurons (Fig. 31, bottom).

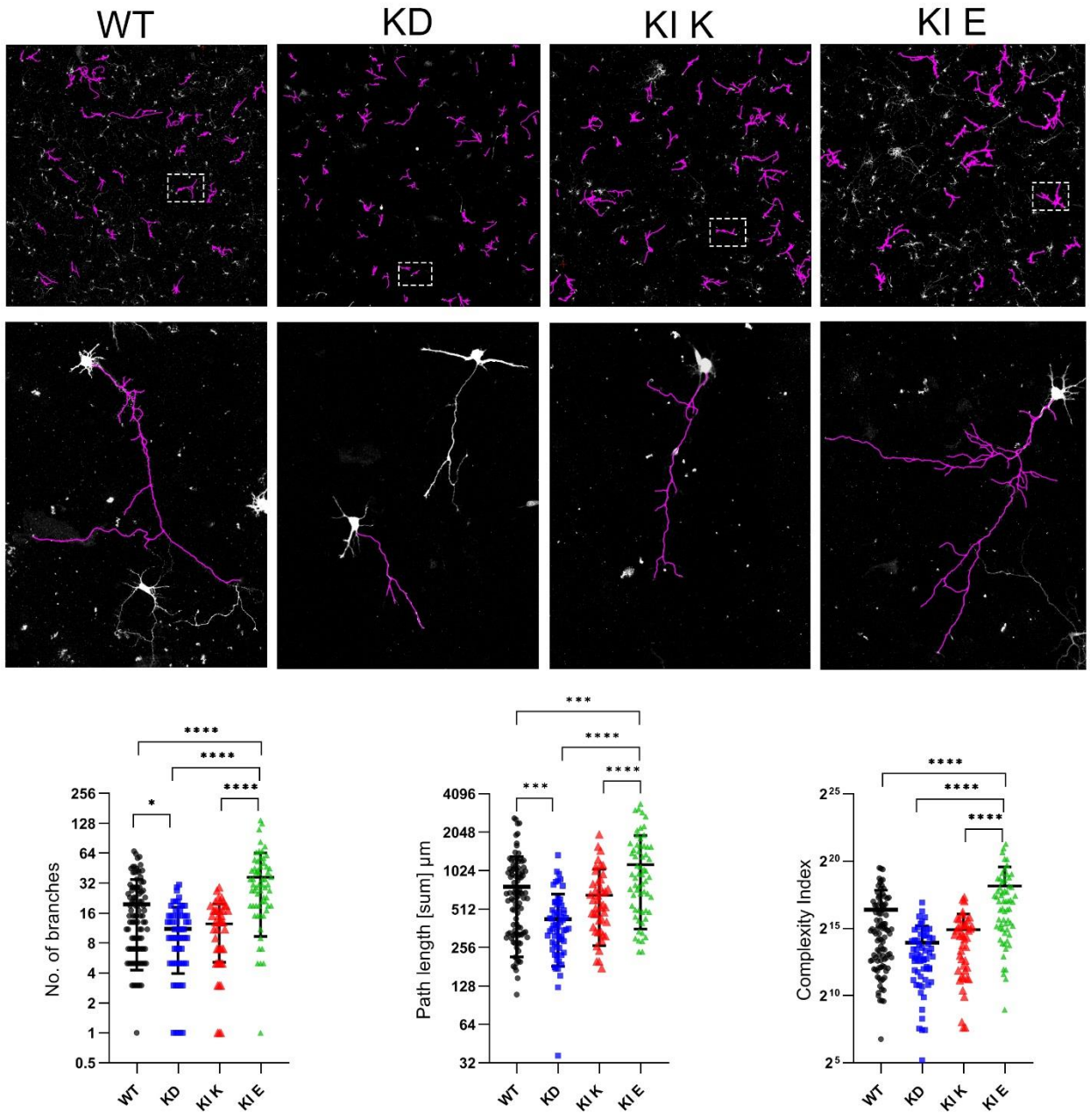

Figure 31

Axon tracing of hippocampal culture at DIV4 by Simple Neurite Tracing in purple (Top). The complexity of axonal arborization was determined by analysing the number of branches, the total length of axons and the complexity index. (N= 97 (WT), 61 (*KD*), 44 (*KI* K), 62 (*KI* E); Tukey's multiple comparisons test: *<0.05 ** <0.01 ***<0.001 ****<0.0001) (Bottom).

Taken together these results suggest a role of CYFIP2 protein in the axonal maturation processes and show the impact of *CYFIP2* K/E RNA editing process in regulating the spreading of neuronal axon during first stages of *in vitro* development.

4.10 Study of spine frequency of hippocampal primary neurons

Actin dynamics are essential for synaptic function, spine formation, and plasticity (Citri & Malenka, 2008). Dendritic spines are highly dynamic membranous protrusions on postsynaptic dendrites, which have a rich F-actin cytoskeleton (Shah & Rossie, 2018). Given that, we decided to apply our neuronal model to investigate if CYFIP2 K/E editing regulation is involved in spine dynamics. Hippocampal cells were cultured for 17 days until the spine structure could be considered as mature and functional. During this time, endogenous CYFIP2 was silenced by lentiviral shRNA, and CYFIP2 K/E variants were expressed constitutively by lentiviral transduction. Cells are fixed and immunofluorescence with α-HA antibody was performed to visualise the expression of the transgene. By confocal microscopy we acquired a GFP signal of the cells that is expressed concurrently with shRNA. This signal, besides providing a marker for the endogenous CYFIP2 protein's silencing, has been used to reconstruct the shape of neuronal cells and to analyse the frequency of spines. We examine a minimum of 17 secondary dendrites from each experimental group, manually counting the number of spines on each one.

As it is possible to observe in Figure 32, the frequency of the spines, which is the number of spines for each ten micrometres in length of the secondary dendrite, significantly changed among the three different experimental groups (One way ANOVA $p<0,001$). In particular, the silencing of the CYFIP2 protein (*KD*), shows a decrease in the spine frequency compared to WT cells. (WT mean=3.65 +/- 0.2262; *KD* mean= 2.06 +/- 0.157; Tukey's multiple comparisons test WT vs. *KD* $p<0.0001$). This decrease remains similar when we induce in the cells the expression of the K variant (K mean=2.499 +/- 0.1205; WT vs. K $p<0.0007$) indicating that the physiological frequency of spines is not recovered after the expression of the CYFIP2 K variant; (*KD* vs. K ns $p<0.3832$). Conversely, this parameter was completely restored after the expression of the CYFIP2 E variant (E mean=3.822 +/-0.2558; *KD* vs. E $p<0.0001$). This difference resulted to be statistically significant also between K and E groups (K vs. E $p<0.0001$).

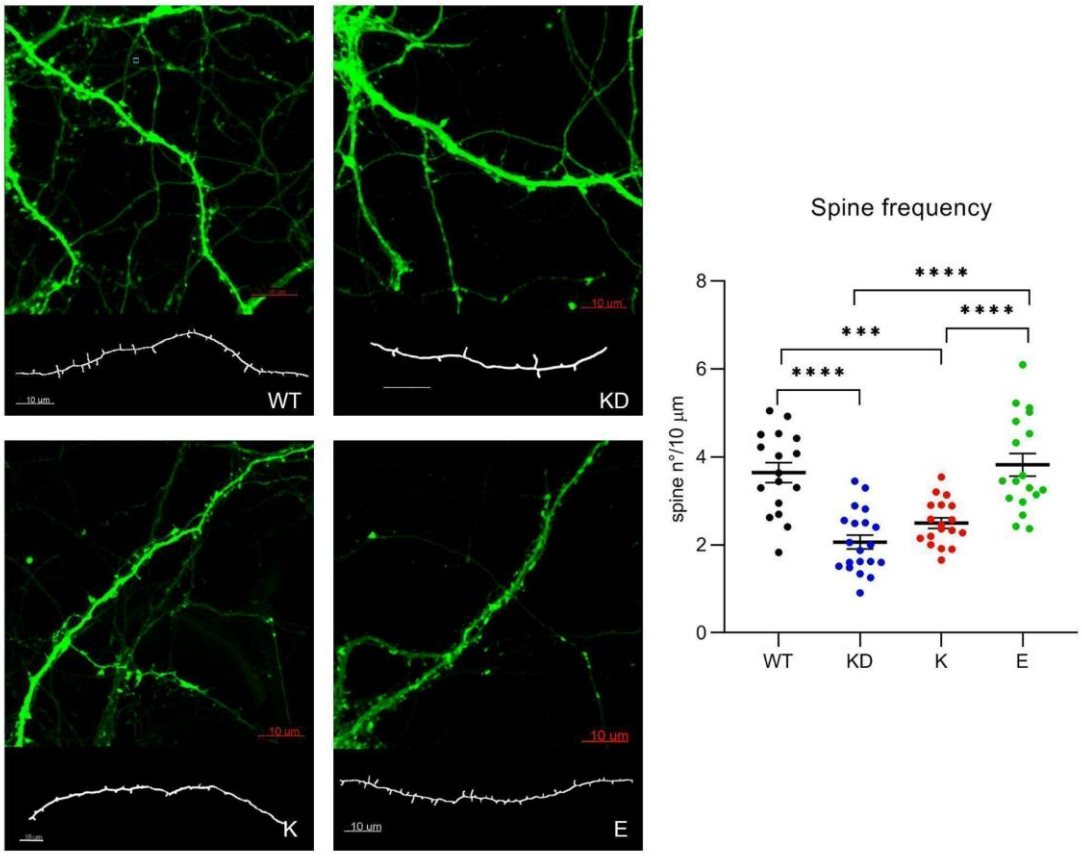

Figure 32

Particular of secondary dendrites of hippocampal cells at DIV18 captured by confocal microscopy. GFP protein signal visible in green, represents a marker of CYFIP2 down-regulation. In white is visible the reconstruction of dendrites and spine structures by imageJ (left). Distribution of spine frequency of different populations of analysed cells (right) (N= 17 (WT), 20 (*KD*), 18 (*KI* K), 18 (*KI* E); (Tukey's multiple comparisons test: ***<0.001 ****<0.0001).

Taken together, the results obtained suggest a clear role of CYFIP2 K/E RNA editing process in regulating the spinogenesis process in the hippocampal *in vitro* model.

5 DISCUSSION

In mammals, the most common type of RNA editing reaction is A to I (Maas et al., 2003), catalysed by ADAR enzymes that are able to bind to double stranded RNA (dsRNA) and modify the A nucleotide into I by deamination.

ADAR enzymes edit the mammalian transcriptome at millions of different sites. The majority of them are found in intronic retrotransposons like ALU-inverted repeats, non-coding sequences like 3′ and 5′ untranslated regions (UTRs) and other retrotransposons (Daniel et al., 2015). If the nucleotide being edited is within a coding sequence of mRNA (re-coding editing), during translation the ribosomes will interpret the inosine as a guanosine, altering the meaning of the RNA codon. A-to-I RNA editing may therefore significantly improve the transcriptome and proteome diversity.

Numerous re-coding sites affect transcripts crucial for neuronal function and are phylogenetically conserved (Behm & Öhman, 2016). In the CNS RNA editing controls the transcription, splicing, and subcellular localization of mRNAs (Behm & Öhman, 2016; La Via et al., 2013; Shimokawa et al., 2013). By allowing the same coding sequence to generate different mRNA and products, these base-specific modifications exponentially increase the variety of RNA sequences and increase the functioning of numerous brain-expressed genes. RNA editing in CNS have impact on essential neurodevelopmental processes, including actin cytoskeletal remodelling at excitatory synapses (Behm & Öhman, 2016; Wahlstedt et al., 2009), regulation of gating kinetics of inhibitory receptors (Behm & Öhman, 2016; Higuchi et al., 2000) and modulation of neurotransmission at inhibitory synapses (Behm & Öhman, 2016; Sommer et al., 1991). Moreover, human cortex development is dynamically modulated by RNA editing sites (Hwang et al., 2016), with significant increases in editing levels between mid-fetal development and infancy. Non-human primates and murine cortical development models share these profiles, revealing an evolutionary function selection (Wahlstedt et al., 2009). Although the number of known editing sites has grown thanks to the expansion of RNA-sequencing datasets, most of the functional significance of these regulations is still unclear.

CYFIP2 is one of these neuro-specific transcripts that undergoes RNA editing (Levanon et al., 2005). The re-coding reaction occurs in the CDS and results in K→E substitution at amino acid 320 and its functional meaning is still unknown. Our research will make a first effort to elucidate the role of this regulation.

Our results show that CYFIP2 RNA editing reaction increases during neural development in a manner similar to other edited neuro-specific transcripts and it is specifically regulated in different brain areas, suggesting a role during neuronal development and function. The decrease of CYFIP2 editing levels in hippocampal cultures treated with glutamate, suggests that this site is functional and can be modulated by neuronal activity.

CYFIP2 protein is a fundamental component of Wave Regulatory Complex (WRC), a key hub for signalling between the plasma membrane and actin in a variety of functions. In its basal state, the WRC is inactive in the cytosol. After various upstream signals arising from growth factors, WRC can be recruited to the specific membrane regions where it will activate the Arp2/3 complex to promote actin polymerization (Abdul-Manan et al., 1999; Rottner et al., 2021). The interaction of Rac1 with the WRC is the primary driver of the complex activation. The active form of Rac (Rac-GTP) binds to the two sites of WRC (A and D) present in the CYFIP2 structure (or CYFIP1), and drives a series of conformational changes in WRC structure that leads to a release from the activator VCA domain which is free to activate the Arp2/3 complex to promote actin polymerization (Schaks et al., 2018).

To try to understand if the K→E amino acid substitution that takes place after CYFIP2 RNA editing reaction, might influence the stability of WRC and afterward the dynamic of its activation, we apply a protein stability and flexibility changes analysis to the WRC model. The results obtained indicate that the edited variant (E) might lead to a destabilisation of the inactive state of WRC. Since the interaction of Rac-GTP with WRC induces a CYFIP2 conformational change, leading to releases of the activatory VCA region of WAVE protein, it is possible to interpret the destabilising effect induced by the presence of the edited variant (E) into the inactive WRC, as a gain of function in the ability of WRC to activate the Arp2/3 complex, even in the absence of external activating inputs generated by Rac-GTP binding after growth factor stimulation.

Analysing the conservation rate of CYFIP2 protein in different species, we found that CYFIP2 protein shows a high rate of conservation between different species. Furthermore, observing the conservation of the amino acid residue present at the position subject to RNA editing, it appears evident how both Lysine (K) and Glutamate (E) are present during evolution. These findings suggest that both amino acids in this particular position of the CYFIP2 protein are tolerated and possibly contribute to the protein's physiology.

In order to investigate if CYFIP2 K/E RNA editing regulation can be implicated in the control of actin dynamics, we use CYFIP2 *KO* neuroblastoma cell lines as an *in vitro* model of cell migration.

It is well established from the literature that inhibition of lamellipodia through blocking WRC or Arp2/3 complex functionality promotes formation of plasma membrane blebs in various cell types in distinct organisms (Suraneni et al., 2012). It is also clearly evident from our findings that after CYFIP2 gene knockdown, SH-SY5Y cells lose their characteristic neuroblast-like phenotype, exhibiting a striking morphological change with the formation of cell blebs on the plasma membrane. *KO* cells showed a completely different actin filaments organisation compared to WT cells. To confirm the implication of CYFIP2 protein in actin cytoskeleton organisation, we create two stable SH-SY5Y *CYFIP2 KI* cell lines, one expressing the unedited CYFIP2 K variants one the edited CYFIP2 E variant. As expected, the alteration in morphological phenotype can be reverted when both CYFIP2 K/E variants are overexpressed.

Since the actin polymerization process is closely related to cell migration, we investigate if CYFIP2 K/E variants can have different impact on this process using a "gap closure migration assay". Our results showed differences of the edited and unedited CYFIP2 proteins in regulating cellular migration. In particular, the edited variant (CYFIP2-E) has a stronger capability to migrate and to invade the experimental wound. We analysed the migration ability of cells, applying two experimental conditions: serum starvation, in which WRC is inactive, and under growth factors stimulation where WRC is active. It is interesting to note that cells that overexpress the E form of the CYFIP2 protein have a markedly improved potential to migrate under conditions of serum deprivation. Altogether these data can indicate that the editing reaction is involved in the acting dynamic underlining cellular migration and the edited variant of CYFIP2 protein appears to present a gain of function in his ability to activate the WRC, even in the absence of external activating stimuli derived from growth factors. These results are in line with the stability variations of the WRC complex observed in the model predicted from the bioinformatic tool.

Since CYFIP2 protein is mainly expressed in neurons (Zhang et al., 2019) and the K/E RNA editing reaction is active only in the central nervous system, we investigate the role of CYFIP2 K/E variants on neuronal development. For this purpose, we use a model of neuronal differentiation based on the application on SH-SY5Y cells of retinoic acid and brain-derived neurotrophic factor (Hromadkova et al., 2020) to monitor the conversion of undifferentiated cells into neuron-like cells. Differentiated WT cells assume a characteristic neurite-like morphology but in contrast, CYFIP2 *KO* cells display a distinctive fibroblast-like morphology with a non-polarized appearance and large soma. This evidence, suggesting the involvement of CYFIP2 protein in the process of neuronal development, is confirmed when we differentiate the *CYFIP2 KI* cell lines. We observe a complete restoration in the ability of neurite development in both *CYFIP2 KI* cell populations (K/E).

Since both the CYFIP2 K and E variants have the same phenotypic effect in this experimental model, we use hippocampal primary culture to test if the two editing variants may impact neuronal maturation in different manners. Literature data show how CYFIP2 is involved in the growth and sorting of retinal ganglion cells axons (Cioni et al., 2018). For this reason, we initially focused on the early stages of neuronal maturation, analysing neuronal axon length and complexity during the first days of *in vitro* neuronal development. Hippocampal neurons were co-transducted with lentiviral particles expressing CYFIP2 K or E variants together with lentivirus expressing shRNA to downregulate endogenous CYFIP2 protein, in order to assess the impact of RNA editing alteration, excluding the effect of endogenous protein. To validate our model of *CYFIP2* RNA editing modulation, we decided to evaluate the real amount of *CYFIP2* editing variant expressed in our experimental groups through Sanger sequencing. The CYFIP2 K/E editing percentage can be interpreted as a function of the relative amount of CYFIP2 K or E variant proteins present in the cells. As expected, the overexpression of the unedited K variant decreased the amount of editing while the K variant increased its level versus control. Increasing the expression of unedited CYFIP2 variant (K), leads to a decrease of complexity of axon development. Conversely, an increase of edited variant expression (E) results in a rise of axon complexity.

Dendritic spines are highly dynamic membranous protrusions on postsynaptic dendrites, rich in F-actin cytoskeleton (Shah & Rossie, 2018). Since synaptic function like spine development and spine plasticity, both depends on actin dynamics (Citri & Malenka, 2008), we decided to apply our neuronal model to investigate if CYFIP2 K/E editing regulation is involved in this fundamental process of neuronal physiology. To this purpose, we measure the frequency of the spines of the secondary dendrite of *in vitro* hippocampal neurons. The silencing of the CYFIP2 protein shows a decrease in the spine frequency compared to WT cells. This decrease remains similar when we induce in the cells the expression of the K variant indicating that the physiological frequency of spines is not recovered after the expression of the CYFIP2 K variant. Conversely, this parameter was completely restored after the expression of the CYFIP2 E variant.

Taken together these results suggest a clear role of *CYFIP2* K/E RNA editing process in regulating both the outgrowth of neuronal axon during first stages of *in vitro* development and the process of spinogenesis in the in the subsequent stages of development of *in vitro* hippocampal cells. This correlation can be observed in Figure 33.

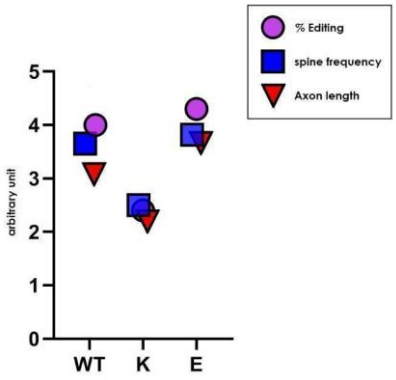

Figure 33

Correlation between the relative presence of unedited (K) and edited (E) variants of CYFIP2 protein with spine frequency and axon complexity in neuronal hippocampal culture.

Our findings suggest that the edited (E) variant of the CYFIP2 protein, when present within the WRC, gives a gain of function in the ability to activate the WRC even in the absence of external activating stimuli derived from growth factors. This hypothesis is summarised in Figure 34.

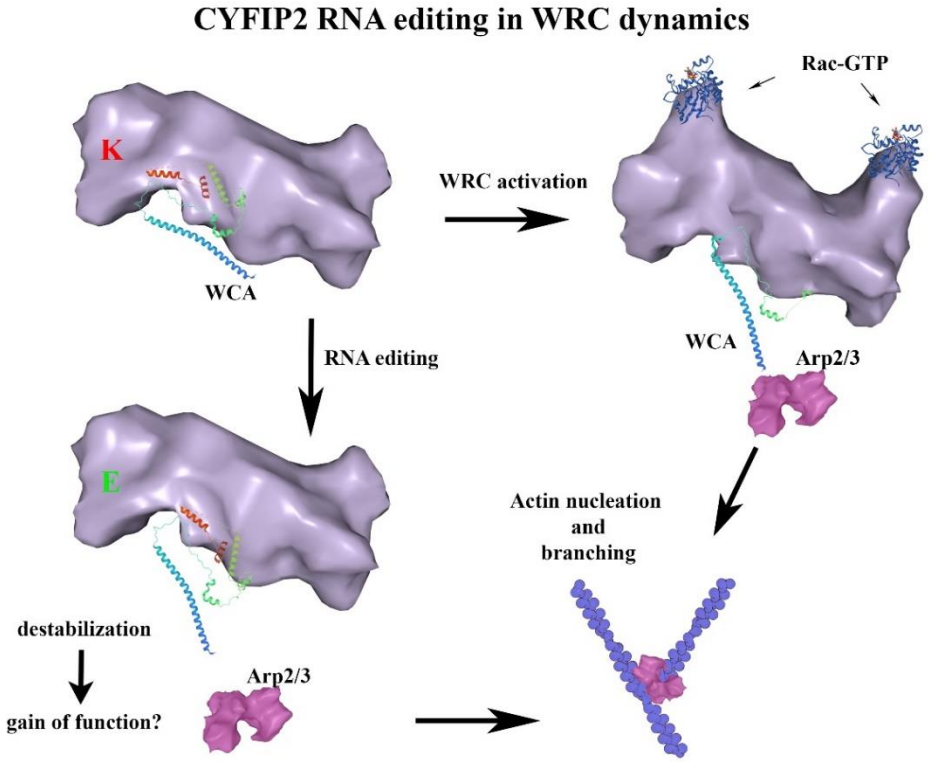

Figure 34

Schematic representation of CYFIP2 K/E RNA editing function in WRC dynamics

The onset of mutations under the pressure of evolution, can result in an improvement in the activity of biological processes crucial for complex systems like the central nervous system. Because epi-transcriptomic A-to-I RNA editing can be temporally modulated to accurately modify the functions of neuronal genes throughout brain development, it can be interpreted as a favourable process with respect to the A-to-G gene mutation in organisms. It is possible that RNA editing mediates numerous layers of controls necessary to build a sophisticated organ system like the brain. An increasing amount of evidence supports this idea, showing how RNA editing has a crucial role in the regulation of the central nervous system physiology (Tariq & Jantsch, 2012). During the process of neural differentiation and maturation and in all stages of brain development, from the embryo to the development of adult tissues, the levels of RNA editing of important neuro-specific transcripts dynamically change. Literature shows besides how abnormal RNA editing control contributes to the pathogenesis of neurological diseases. Deep sequencing has dramatically increased the number of editing sites now known, but in a portion of these sites it is not yet clear how RNA editing events affect protein functions (Chalk et al., 2019).

Our research has uncovered for the first time how actin dynamic processes are related to the *CYFIP2* K/E RNA editing process in the neuronal development and function. Further studies are necessary to determine whether this process is equally relevant *in vivo*.

Besides to being a component of the WRC complex implicated in actin dynamics, the CYFIP2 protein was also physically associated to the FMRP protein, one of the most important RNA-binding protein considerate to be a master regulator of protein translation of RNAs essential for neuronal physiology.

Given that the regulation of protein synthesis operated by FMRP is a fundamental process in the modulation of synaptic activity and it is strictly related to the actin dynamic rearrangement that occurred inside the dendritic spine, it is fundamental to investigate whether RNA editing of *CYFIP2* may be implicated in this process.

6 BIBLIOGRAPHY

Abdul-Manan, N., Aghazadeh, B., Liu, G. A., Majumdar, A., Ouerfelli, O., Siminovitch, K. A., & Rosen, M. K. (1999). Structure of Cdc42 in complex with the GTPase-binding domain of the 'Wiskott-Aldrich syndrome' protein. *Nature*, *399*(6734), Article 6734. https://doi.org/10.1038/20726

Abekhoukh, S., & Bardoni, B. (2014). CYFIP family proteins between autism and intellectual disability: Links with Fragile X syndrome. *Frontiers in Cellular Neuroscience*, *8*, 81. https://doi.org/10.3389/fncel.2014.00081

Abo, A., Pick, E., Hall, A., Totty, N., Teahan, C. G., & Segal, A. W. (1991). Activation of the NADPH oxidase involves the small GTP-binding protein p21rac1. *Nature*, *353*(6345), 668–670. https://doi.org/10.1038/353668a0

Alekhina, O., Burstein, E., & Billadeau, D. D. (2017). Cellular functions of WASP family proteins at a glance. *Journal of Cell Science*, *130*(14), Article 14. https://doi.org/10.1242/jcs.199570

Arshadi, C., Günther, U., Eddison, M., Harrington, K. I. S., & Ferreira, T. A. (2021). SNT: A unifying toolbox for quantification of neuronal anatomy. *Nature Methods*, *18*(4), 374–377. https://doi.org/10.1038/s41592-021-01105-7

Bagni, C., & Oostra, B. A. (2013). Fragile X syndrome: From protein function to therapy. *American Journal of Medical Genetics. Part A*, *161A*(11), 2809–2821. https://doi.org/10.1002/ajmg.a.36241

Bagni, C., & Zukin, R. S. (2019). A Synaptic Perspective of Fragile X Syndrome and Autism Spectrum Disorders. *Neuron*, *101*(6), 1070–1088. https://doi.org/10.1016/j.neuron.2019.02.041

Bajad, P., Jantsch, M. F., Keegan, L., & O'Connell, M. (2017). A to I editing in disease is not fake news. *RNA Biology*, *14*(9), 1223–1231. https://doi.org/10.1080/15476286.2017.1306173

Barbon, A., & Magri, C. (2020). RNA Editing and Modifications in Mood Disorders. *Genes*, *11*(8), 872. https://doi.org/10.3390/genes11080872

Barbon, A., Vallini, I., La Via, L., Marchina, E., & Barlati, S. (2003). Glutamate receptor RNA editing: A molecular analysis of GluR2, GluR5 and GluR6 in human brain tissues and in NT2 cells following in vitro neural differentiation. *Brain Research. Molecular Brain Research*, *117*(2), 168–178. https://doi.org/10.1016/s0169-328x(03)00317-6

Bass, B. L. (2002). RNA editing by adenosine deaminases that act on RNA. *Annual Review of Biochemistry*, *71*, 817–846. https://doi.org/10.1146/annurev.biochem.71.110601.135501

Bazak, L., Haviv, A., Barak, M., Jacob-Hirsch, J., Deng, P., Zhang, R., Isaacs, F. J., Rechavi, G., Li, J. B., Eisenberg, E., & Levanon, E. Y. (2014). A-to-I RNA editing occurs at over a hundred million genomic sites, located in a majority of human genes. *Genome Research*, *24*(3), 365–376. https://doi.org/10.1101/gr.164749.113

Begemann, A., Sticht, H., Begtrup, A., Vitobello, A., Faivre, L., Banka, S., Alhaddad, B., Asadollahi, R., Becker, J., Bierhals, T., Brown, K. E., Bruel, A.-L., Brunet, T., Carneiro, M., Cremer, K., Day, R., Denommé-Pichon, A.-S., Dyment, D. A., Engels, H., … Rauch, A. (2021). New insights into the clinical and molecular spectrum of the novel CYFIP2-related neurodevelopmental disorder and impairment of the WRC-mediated actin dynamics. *Genetics in Medicine: Official Journal of the American College of Medical Genetics*, *23*(3), 543–554. https://doi.org/10.1038/s41436-020-01011-x

Behm, M., & Öhman, M. (2016). RNA Editing: A Contributor to Neuronal Dynamics in the Mammalian Brain. *Trends in Genetics: TIG*, *32*(3), 165–175. https://doi.org/10.1016/j.tig.2015.12.005

Biembengut, Í. V., Shigunov, P., Frota, N. F., Lourenzoni, M. R., & de Souza, T. A. C. B. (2022). Molecular Dynamics of CYFIP2 Protein and Its R87C Variant Related to Early Infantile Epileptic Encephalopathy. *International Journal of Molecular Sciences*, *23*(15), 8708. https://doi.org/10.3390/ijms23158708

Biembengut, Í. V., Silva, I. L. Z., Souza, T. de A. C. B. de, & Shigunov, P. (2021). Cytoplasmic FMR1 interacting protein (CYFIP) family members and their function in neural development and disorders. *Molecular Biology Reports*, *48*(8), 6131–6143. https://doi.org/10.1007/s11033-021-06585-6

Bonini, D., Filippini, A., La Via, L., Fiorentini, C., Fumagalli, F., Colombi, M., & Barbon, A. (2015). Chronic glutamate treatment selectively modulates AMPA RNA editing and ADAR expression and activity in primary cortical neurons. *RNA Biology*, *12*(1), 43–53. https://doi.org/10.1080/15476286.2015.1008365

Breen, M. S., Dobbyn, A., Li, Q., Roussos, P., Hoffman, G. E., Stahl, E., Chess, A., Sklar, P., Li, J. B., Devlin, B., Buxbaum, J. D., & CommonMind Consortium. (2019). Global landscape and genetic regulation of RNA editing in cortical samples from individuals with schizophrenia. *Nature Neuroscience*, *22*(9), 1402–1412. https://doi.org/10.1038/s41593-019-0463-7

Brümmer, A., Yang, Y., Chan, T. W., & Xiao, X. (2017). Structure-mediated modulation of mRNA abundance by A-to-I editing. *Nature Communications*, *8*(1), 1255. https://doi.org/10.1038/s41467-017-01459-7

Bryant, C. D., Zhang, N. N., Sokoloff, G., Fanselow, M. S., Ennes, H. S., Palmer, A. A., & McRoberts, J. A. (2008). Behavioral differences among C57BL/6 substrains: Implications for transgenic and knockout studies. *Journal of Neurogenetics*, *22*(4), 315–331. https://doi.org/10.1080/01677060802357388

Campellone, K. G., & Welch, M. D. (2010). A nucleator arms race: Cellular control of actin assembly. *Nature Reviews. Molecular Cell Biology*, *11*(4), Article 4. https://doi.org/10.1038/nrm2867

Chalk, A. M., Taylor, S., Heraud-Farlow, J. E., & Walkley, C. R. (2019). The majority of A-to-I RNA editing is not required for mammalian homeostasis. *Genome Biology*, *20*(1), 268. https://doi.org/10.1186/s13059-019-1873-2

Charras, G. T., Yarrow, J. C., Horton, M. A., Mahadevan, L., & Mitchison, T. J. (2005). Non-equilibration of hydrostatic pressure in blebbing cells. *Nature*, *435*(7040), 365–369. https://doi.org/10.1038/nature03550

Chen, B., Chou, H.-T., Brautigam, C. A., Xing, W., Yang, S., Henry, L., Doolittle, L. K., Walz, T., & Rosen, M. K. (2017). Rac1 GTPase activates the WAVE regulatory complex through two distinct binding sites. *ELife*, *6*, e29795. https://doi.org/10.7554/eLife.29795

Chen, Z., Borek, D., Padrick, S. B., Gomez, T. S., Metlagel, Z., Ismail, A. M., Umetani, J., Billadeau, D. D., Otwinowski, Z., & Rosen, M. K. (2010). Structure and control of the actin regulatory WAVE complex. *Nature*, *468*(7323), 533–538. https://doi.org/10.1038/nature09623

Chilibeck, K. A., Wu, T., Liang, C., Schellenberg, M. J., Gesner, E. M., Lynch, J. M., & MacMillan, A. M. (2006). FRET analysis of in vivo dimerization by RNA-editing enzymes. *The Journal of Biological Chemistry*, *281*(24), 16530–16535. https://doi.org/10.1074/jbc.M511831200

Cioni, J.-M., Wong, H. H.-W., Bressan, D., Kodama, L., Harris, W. A., & Holt, C. E. (2018). Axon-Axon Interactions Regulate Topographic Optic Tract Sorting via CYFIP2-Dependent WAVE Complex Function. *Neuron*, *97*(5), 1078-1093.e6. https://doi.org/10.1016/j.neuron.2018.01.027

Citri, A., & Malenka, R. C. (2008). Synaptic plasticity: Multiple forms, functions, and mechanisms. *Neuropsychopharmacology: Official Publication of the American College of Neuropsychopharmacology*, *33*(1), Article 1. https://doi.org/10.1038/sj.npp.1301559

Concordet, J.-P., & Haeussler, M. (2018). CRISPOR: Intuitive guide selection for CRISPR/Cas9 genome editing experiments and screens. *Nucleic Acids Research*, *46*(W1), W242–W245. https://doi.org/10.1093/nar/gky354

Cong, L., Ran, F. A., Cox, D., Lin, S., Barretto, R., Habib, N., Hsu, P. D., Wu, X., Jiang, W., Marraffini, L. A., & Zhang, F. (2013). Multiplex genome engineering using CRISPR/Cas systems. *Science (New York, N.Y.)*, *339*(6121), 819–823. https://doi.org/10.1126/science.1231143

Contreras, E. G., Egger, B., Gold, K. S., & Brand, A. H. (2018). Dynamic Notch signalling regulates neural stem cell state progression in the Drosophila optic lobe. *Neural Development*, *13*(1), 25. https://doi.org/10.1186/s13064-018-0123-8

Daniel, C., Behm, M., & Öhman, M. (2015). The role of Alu elements in the cis-regulation of RNA processing. *Cellular and Molecular Life Sciences: CMLS*, *72*(21), 4063–4076. https://doi.org/10.1007/s00018-015-1990-3

De Rubeis, S., Pasciuto, E., Li, K. W., Fernández, E., Di Marino, D., Buzzi, A., Ostroff, L. E., Klann, E., Zwartkruis, F. J. T., Komiyama, N. H., Grant, S. G. N., Poujol, C., Choquet, D., Achsel, T., Posthuma, D., Smit, A. B., & Bagni, C. (2013). CYFIP1 coordinates mRNA translation and cytoskeleton remodeling to ensure proper dendritic spine formation. *Neuron*, *79*(6), 1169–1182. https://doi.org/10.1016/j.neuron.2013.06.039

Ding, B., Yang, S., Schaks, M., Liu, Y., Brown, A. J., Rottner, K., Chowdhury, S., & Chen, B. (2022). Structures reveal a key mechanism of WAVE regulatory complex activation by Rac1 GTPase. *Nature Communications*, *13*(1), 5444. https://doi.org/10.1038/s41467-022-33174-3

Domínguez-Iturza, N., Lo, A. C., Shah, D., Armendáriz, M., Vannelli, A., Mercaldo, V., Trusel, M., Li, K. W., Gastaldo, D., Santos, A. R., Callaerts-Vegh, Z., D'Hooge, R., Mameli, M., Van der Linden, A., Smit, A. B., Achsel, T., & Bagni, C. (2019). The autism- and schizophrenia-associated protein CYFIP1 regulates bilateral brain connectivity and behaviour. *Nature Communications*, *10*(1), 3454. https://doi.org/10.1038/s41467-019-11203-y

Dziunycz, P. J., Neu, J., Lefort, K., Djerbi, N., Freiberger, S. N., Iotzova-Weiss, G., French, L. E., Dotto, G.-P., & Hofbauer, G. F. (2017). CYFIP1 is directly controlled by NOTCH1 and down-regulated in cutaneous squamous cell carcinoma. *PloS One*, *12*(4), e0173000. https://doi.org/10.1371/journal.pone.0173000

Egger, B., Gold, K. S., & Brand, A. H. (2010). Notch regulates the switch from symmetric to asymmetric neural stem cell division in the Drosophila optic lobe. *Development (Cambridge, England)*, *137*(18), 2981–2987. https://doi.org/10.1242/dev.051250

Eran, A., Li, J. B., Vatalaro, K., McCarthy, J., Rahimov, F., Collins, C., Markianos, K., Margulies, D. M., Brown, E. N., Calvo, S. E., Kohane, I. S., & Kunkel, L. M. (2013). Comparative RNA editing in autistic and neurotypical cerebella. *Molecular Psychiatry*, *18*(9), 1041–1048. https://doi.org/10.1038/mp.2012.118

Filippini, A., Bonini, D., Giacopuzzi, E., La Via, L., Gangemi, F., Colombi, M., & Barbon, A. (2018). Differential Enzymatic Activity of Rat ADAR2 Splicing Variants Is Due to Altered Capability to Interact with RNA in the Deaminase Domain. *Genes*, *9*(2), 79. https://doi.org/10.3390/genes9020079

Filippini, A., Bonini, D., Lacoux, C., Pacini, L., Zingariello, M., Sancillo, L., Bosisio, D., Salvi, V., Mingardi, J., La Via, L., Zalfa, F., Bagni, C., & Barbon, A. (2017). Absence of the Fragile X Mental Retardation Protein results in defects of RNA editing of neuronal mRNAs in mouse. *RNA Biology*, *14*(11), 1580–1591. https://doi.org/10.1080/15476286.2017.1338232

Fricano-Kugler, C., Gordon, A., Shin, G., Gao, K., Nguyen, J., Berg, J., Starks, M., & Geschwind, D. H. (2019). CYFIP1 overexpression increases fear response in mice but does not affect social or repetitive behavioral phenotypes. *Molecular Autism*, *10*, 25. https://doi.org/10.1186/s13229-019-0278-0

Gabay, O., Shoshan, Y., Kopel, E., Ben-Zvi, U., Mann, T. D., Bressler, N., Cohen-Fultheim, R., Schaffer, A. A., Roth, S. H., Tzur, Z., Levanon, E. Y., & Eisenberg, E. (2022). Landscape of adenosine-to-inosine RNA recoding across human tissues. *Nature Communications*, *13*(1), 1184. https://doi.org/10.1038/s41467-022-28841-4

Gardner, O. K., Wang, L., Van Booven, D., Whitehead, P. L., Hamilton-Nelson, K. L., Adams, L. D., Starks, T. D., Hofmann, N. K., Vance, J. M., Cuccaro, M. L., Martin, E. R., Byrd, G. S., Haines, J. L., Bush, W. S., Beecham, G. W., Pericak-Vance, M. A., & Griswold, A. J. (2019). RNA editing alterations in a multi-ethnic Alzheimer disease cohort converge on immune and endocytic molecular pathways. *Human Molecular Genetics*, *28*(18), 3053–3061. https://doi.org/10.1093/hmg/ddz110

Gautreau, A., Ho, H. H., Li, J., Steen, H., Gygi, S. P., & Kirschner, M. W. (2004). Purification and architecture of the ubiquitous Wave complex. *Proceedings of the National Academy of Sciences of the United States of America*, *101*(13), Article 13. https://doi.org/10.1073/pnas.0400628101

Gerber, A., O'Connell, M. A., & Keller, W. (1997). Two forms of human double-stranded RNA-specific editase 1 (hRED1) generated by the insertion of an Alu cassette. *RNA (New York, N.Y.)*, *3*(5), 453–463.

Ghosh, A., Mizuno, K., Tiwari, S. S., Proitsi, P., Gomez Perez-Nievas, B., Glennon, E., Martinez-Nunez, R. T., & Giese, K. P. (2020). Alzheimer's disease-related dysregulation of mRNA translation causes key pathological features with ageing. *Translational Psychiatry*, *10*(1), 192. https://doi.org/10.1038/s41398-020-00882-7

Goldeck, M., Gopal, A., Jantsch, M. F., Mansouri Khosravi, H. R., Rajendra, V., & Vesely, C. (2022). How RNA editing keeps an I on physiology. *American Journal of Physiology. Cell Physiology*, *323*(5), C1496–C1511. https://doi.org/10.1152/ajpcell.00191.2022

Guo, F., Cancelas, J. A., Hildeman, D., Williams, D. A., & Zheng, Y. (2008). Rac GTPase isoforms Rac1 and Rac2 play a redundant and crucial role in T-cell development. *Blood*, *112*(5), 1767–1775. https://doi.org/10.1182/blood-2008-01-132068

Habela, C. W., Yoon, K.-J., Kim, N.-S., Taga, A., Bell, K., Bergles, D. E., Maragakis, N. J., Ming, G.-L., & Song, H. (2020). Persistent Cyfip1 Expression Is Required to Maintain the Adult Subventricular Zone Neurogenic Niche. *The Journal of Neuroscience: The Official Journal of the Society for Neuroscience*, *40*(10), 2015–2024. https://doi.org/10.1523/JNEUROSCI.2249-19.2020

Han, K., Chen, H., Gennarino, V. A., Richman, R., Lu, H.-C., & Zoghbi, H. Y. (2015). Fragile X-like behaviors and abnormal cortical dendritic spines in cytoplasmic FMR1-interacting protein 2-mutant mice. *Human Molecular Genetics*, *24*(7), 1813–1823. https://doi.org/10.1093/hmg/ddu595

Higuchi, M., Maas, S., Single, F. N., Hartner, J., Rozov, A., Burnashev, N., Feldmeyer, D., Sprengel, R., & Seeburg, P. H. (2000). Point mutation in an AMPA receptor gene rescues lethality in mice deficient in the RNA-editing enzyme ADAR2. *Nature*, *406*(6791), 78–81. https://doi.org/10.1038/35017558

Hoeffer, C. A., Sanchez, E., Hagerman, R. J., Mu, Y., Nguyen, D. V., Wong, H., Whelan, A. M., Zukin, R. S., Klann, E., & Tassone, F. (2012). Altered mTOR signaling and enhanced CYFIP2 expression levels in subjects with fragile X syndrome. *Genes, Brain, and Behavior*, *11*(3), 332–341. https://doi.org/10.1111/j.1601-183X.2012.00768.x

Hoover, B. R., Reed, M. N., Su, J., Penrod, R. D., Kotilinek, L. A., Grant, M. K., Pitstick, R., Carlson, G. A., Lanier, L. M., Yuan, L.-L., Ashe, K. H., & Liao, D. (2010). Tau mislocalization to dendritic spines mediates synaptic dysfunction independently of neurodegeneration. *Neuron*, *68*(6), 1067–1081. https://doi.org/10.1016/j.neuron.2010.11.030

Hromadkova, L., Bezdekova, D., Pala, J., Schedin-Weiss, S., Tjernberg, L. O., Hoschl, C., & Ovsepian, S. V. (2020). Brain-derived neurotrophic factor (BDNF) promotes molecular polarization and differentiation of immature neuroblastoma cells into definitive neurons. *Biochimica Et Biophysica Acta. Molecular Cell Research*, *1867*(9), 118737. https://doi.org/10.1016/j.bbamcr.2020.118737

Hsu, P. D., Scott, D. A., Weinstein, J. A., Ran, F. A., Konermann, S., Agarwala, V., Li, Y., Fine, E. J., Wu, X., Shalem, O., Cradick, T. J., Marraffini, L. A., Bao, G., & Zhang, F. (2013). DNA targeting specificity of RNA-guided Cas9 nucleases. *Nature Biotechnology*, *31*(9), 827–832. https://doi.org/10.1038/nbt.2647

Hwang, T., Park, C.-K., Leung, A. K. L., Gao, Y., Hyde, T. M., Kleinman, J. E., Rajpurohit, A., Tao, R., Shin, J. H., & Weinberger, D. R. (2016). Dynamic regulation of RNA editing in human brain development and disease. *Nature Neuroscience*, *19*(8), 1093–1099. https://doi.org/10.1038/nn.4337

Jackson, R. S., Cho, Y.-J., Stein, S., & Liang, P. (2007). CYFIP2, a direct p53 target, is leptomycin-B sensitive. *Cell Cycle (Georgetown, Tex.)*, *6*(1), 95–103. https://doi.org/10.4161/cc.6.1.3665

Keegan, L. P., Gallo, A., & O'Connell, M. A. (2001). The many roles of an RNA editor. *Nature Reviews. Genetics*, *2*(11), 869–878. https://doi.org/10.1038/35098584

Kim, G. H., Zhang, Y., Kang, H. R., Lee, S.-H., Shin, J., Lee, C. H., Kang, H., Ma, R., Jin, C., Kim, Y., Kim, S. Y., Kwon, S.-K., Choi, S.-Y., Lee, K. J., & Han, K. (2020). Altered presynaptic function and number of mitochondria in the medial prefrontal cortex of adult Cyfip2 heterozygous mice. *Molecular Brain*, *13*(1), 123. https://doi.org/10.1186/s13041-020-00668-4

Kim, S. K. (2000). Cell polarity: New PARtners for Cdc42 and Rac. *Nature Cell Biology*, *2*(8), E143-145. https://doi.org/10.1038/35019620

Kirkpatrick, S. L., Goldberg, L. R., Yazdani, N., Babbs, R. K., Wu, J., Reed, E. R., Jenkins, D. F., Bolgioni, A. F., Landaverde, K. I., Luttik, K. P., Mitchell, K. S., Kumar, V., Johnson, W. E., Mulligan, M. K., Cottone, P., & Bryant, C. D. (2017). Cytoplasmic FMR1-Interacting Protein 2 Is a Major Genetic Factor Underlying Binge Eating. *Biological Psychiatry*, *81*(9), 757–769. https://doi.org/10.1016/j.biopsych.2016.10.021

Kobayashi, K., Kuroda, S., Fukata, M., Nakamura, T., Nagase, T., Nomura, N., Matsuura, Y., Yoshida-Kubomura, N., Iwamatsu, A., & Kaibuchi, K. (1998). P140Sra-1 (specifically Rac1-associated protein) is a novel specific target for Rac1 small GTPase. *The Journal of Biological Chemistry*, *273*(1), 291–295. https://doi.org/10.1074/jbc.273.1.291

Kumar, V., Kim, K., Joseph, C., Kourrich, S., Yoo, S.-H., Huang, H. C., Vitaterna, M. H., de Villena, F. P.-M., Churchill, G., Bonci, A., & Takahashi, J. S. (2013). C57BL/6N mutation in cytoplasmic FMRP interacting protein 2 regulates cocaine response. *Science (New York, N.Y.)*, *342*(6165), 1508–1512. https://doi.org/10.1126/science.1245503

La Via, L., Bonini, D., Russo, I., Orlandi, C., Barlati, S., & Barbon, A. (2013). Modulation of dendritic AMPA receptor mRNA trafficking by RNA splicing and editing. *Nucleic Acids Research*, *41*(1), 617–631. https://doi.org/10.1093/nar/gks1223

Lappalainen, P., Kotila, T., Jégou, A., & Romet-Lemonne, G. (2022). Biochemical and mechanical regulation of actin dynamics. *Nature Reviews. Molecular Cell Biology*, *23*(12), Article 12. https://doi.org/10.1038/s41580-022-00508-4

Lee, Y., Zhang, Y., Kang, H., Bang, G., Kim, Y., Kang, H. R., Ma, R., Jin, C., Kim, J. Y., & Han, K. (2020). Epilepsy- and intellectual disability-associated CYFIP2 interacts with both actin regulators and RNA-binding proteins in the neonatal mouse forebrain. *Biochemical and Biophysical Research Communications*, *529*(1), 1–6. https://doi.org/10.1016/j.bbrc.2020.05.221

Levanon, E. Y., Hallegger, M., Kinar, Y., Shemesh, R., Djinovic-Carugo, K., Rechavi, G., Jantsch, M. F., & Eisenberg, E. (2005). Evolutionarily conserved human targets of adenosine to inosine RNA editing. *Nucleic Acids Research*, *33*(4), 1162–1168. https://doi.org/10.1093/nar/gki239

Lin, J., Liao, S., Li, E., Liu, Z., Zheng, R., Wu, X., & Zeng, W. (2020). CircCYFIP2 Acts as a Sponge of miR-1205 and Affects the Expression of Its Target Gene E2F1 to Regulate Gastric Cancer Metastasis. *Molecular Therapy. Nucleic Acids*, *21*, 121–132. https://doi.org/10.1016/j.omtn.2020.05.007

Maas, S., Rich, A., & Nishikura, K. (2003). A-to-I RNA editing: Recent news and residual mysteries. *The Journal of Biological Chemistry*, *278*(3), 1391–1394. https://doi.org/10.1074/jbc.R200025200

Machesky, L. M., Mullins, R. D., Higgs, H. N., Kaiser, D. A., Blanchoin, L., May, R. C., Hall, M. E., & Pollard, T. D. (1999). Scar, a WASp-related protein, activates nucleation of actin filaments by the Arp2/3 complex. *Proceedings of the National Academy of Sciences of the United States of America*, *96*(7), Article 7. https://doi.org/10.1073/pnas.96.7.3739

Mannion, N. M., Greenwood, S. M., Young, R., Cox, S., Brindle, J., Read, D., Nellåker, C., Vesely, C., Ponting, C. P., McLaughlin, P. J., Jantsch, M. F., Dorin, J., Adams, I. R., Scadden, A. D. J., Ohman, M., Keegan, L. P., & O'Connell, M. A. (2014). The RNA-editing enzyme ADAR1 controls innate immune responses to RNA. *Cell Reports*, *9*(4), 1482–1494. https://doi.org/10.1016/j.celrep.2014.10.041

Mayne, M., Moffatt, T., Kong, H., McLaren, P. J., Fowke, K. R., Becker, K. G., Namaka, M., Schenck, A., Bardoni, B., Bernstein, C. N., & Melanson, M. (2004). CYFIP2 is highly abundant in CD4+ cells from multiple sclerosis patients and is involved in T cell adhesion. *European Journal of Immunology*, *34*(4), 1217–1227. https://doi.org/10.1002/eji.200324726

Michaelsen-Preusse, K., Feuge, J., & Korte, M. (2018). Imbalance of synaptic actin dynamics as a key to fragile X syndrome? *The Journal of Physiology*, *596*(14), 2773–2782. https://doi.org/10.1113/JP275571

Moore, S., Alsop, E., Lorenzini, I., Starr, A., Rabichow, B. E., Mendez, E., Levy, J. L., Burciu, C., Reiman, R., Chew, J., Belzil, V. V., W Dickson, D., Robertson, J., Staats, K. A., Ichida, J. K., Petrucelli, L., Van Keuren-Jensen, K., & Sattler, R. (2019). ADAR2 mislocalization and widespread RNA editing aberrations in C9orf72-mediated ALS/FTD. *Acta Neuropathologica*, *138*(1), 49–65. https://doi.org/10.1007/s00401-019-01999-w

Nakashima, M., Kato, M., Aoto, K., Shiina, M., Belal, H., Mukaida, S., Kumada, S., Sato, A., Zerem, A., Lerman-Sagie, T., Lev, D., Leong, H. Y., Tsurusaki, Y., Mizuguchi, T., Miyatake, S., Miyake, N., Ogata, K., Saitsu, H., & Matsumoto, N. (2018). De novo hotspot variants in CYFIP2 cause early-onset epileptic encephalopathy. *Annals of Neurology*, *83*(4), 794–806. https://doi.org/10.1002/ana.25208

Napoli, I., Mercaldo, V., Boyl, P. P., Eleuteri, B., Zalfa, F., De Rubeis, S., Di Marino, D., Mohr, E., Massimi, M., Falconi, M., Witke, W., Costa-Mattioli, M., Sonenberg, N., Achsel, T., & Bagni, C. (2008). The fragile X syndrome protein represses activity-dependent translation through CYFIP1, a new 4E-BP. *Cell*, *134*(6), 1042–1054. https://doi.org/10.1016/j.cell.2008.07.031

Nicholas, A., de Magalhaes, J. P., Kraytsberg, Y., Richfield, E. K., Levanon, E. Y., & Khrapko, K. (2010). Age-related gene-specific changes of A-to-I mRNA editing in the human brain. *Mechanisms of Ageing and Development*, *131*(6), 445–447. https://doi.org/10.1016/j.mad.2010.06.001

Nishikura, K. (2010). Functions and regulation of RNA editing by ADAR deaminases. *Annual Review of Biochemistry*, *79*, 321–349. https://doi.org/10.1146/annurev-biochem-060208-105251

Noroozi, R., Omrani, M. D., Sayad, A., Taheri, M., & Ghafouri-Fard, S. (2018). Cytoplasmic FMRP interacting protein 1/2 (CYFIP1/2) expression analysis in autism. *Metabolic Brain Disease*, *33*(4), 1353–1358. https://doi.org/10.1007/s11011-018-0249-8

Oguro-Ando, A., Rosensweig, C., Herman, E., Nishimura, Y., Werling, D., Bill, B. R., Berg, J. M., Gao, F., Coppola, G., Abrahams, B. S., & Geschwind, D. H. (2015). Increased CYFIP1 dosage alters cellular and dendritic morphology and dysregulates mTOR. *Molecular Psychiatry*, *20*(9), 1069–1078. https://doi.org/10.1038/mp.2014.124

Orlandi, C., Barbon, A., & Barlati, S. (2012). Activity regulation of adenosine deaminases acting on RNA (ADARs). *Molecular Neurobiology*, *45*(1), 61–75. https://doi.org/10.1007/s12035-011-8220-2

Orlandi, C., La Via, L., Bonini, D., Mora, C., Russo, I., Barbon, A., & Barlati, S. (2011). AMPA receptor regulation at the mRNA and protein level in rat primary cortical cultures. *PloS One*, *6*(9), e25350. https://doi.org/10.1371/journal.pone.0025350

Ozaki, T., & Nakagawara, A. (2011). Role of p53 in Cell Death and Human Cancers. *Cancers*, *3*(1), 994–1013. https://doi.org/10.3390/cancers3010994

Padrick, S. B., Cheng, H.-C., Ismail, A. M., Panchal, S. C., Doolittle, L. K., Kim, S., Skehan, B. M., Umetani, J., Brautigam, C. A., Leong, J. M., & Rosen, M. K. (2008). Hierarchical regulation of WASP/WAVE proteins. *Molecular Cell*, *32*(3), Article 3. https://doi.org/10.1016/j.molcel.2008.10.012

Peng, J., Wang, Y., He, F., Chen, C., Wu, L.-W., Yang, L.-F., Ma, Y.-P., Zhang, W., Shi, Z.-Q., Chen, C., Xia, K., Guo, H., Yin, F., & Pang, N. (2018). Novel West syndrome candidate genes in a Chinese cohort. *CNS Neuroscience & Therapeutics*, *24*(12), 1196–1206. https://doi.org/10.1111/cns.12860

Pollard, T. D. (2016). Actin and Actin-Binding Proteins. *Cold Spring Harbor Perspectives in Biology*, *8*(8), Article 8. https://doi.org/10.1101/cshperspect.a018226

Qian, Y., Guan, T., Tang, X., Huang, L., Huang, M., Li, Y., Sun, H., Yu, R., & Zhang, F. (2011). Astrocytic glutamate transporter-dependent neuroprotection against glutamate toxicity: An in vitro study of maslinic acid. *European Journal of Pharmacology*, *651*(1–3), 59–65. https://doi.org/10.1016/j.ejphar.2010.10.095

Ran, F. A., Hsu, P. D., Wright, J., Agarwala, V., Scott, D. A., & Zhang, F. (2013). Genome engineering using the CRISPR-Cas9 system. *Nature Protocols*, *8*(11), 2281–2308. https://doi.org/10.1038/nprot.2013.143

Ridley, A. J., Paterson, H. F., Johnston, C. L., Diekmann, D., & Hall, A. (1992). The small GTP-binding protein rac regulates growth factor-induced membrane ruffling. *Cell*, *70*(3), 401–410. https://doi.org/10.1016/0092-8674(92)90164-8

Riedmann, E. M., Schopoff, S., Hartner, J. C., & Jantsch, M. F. (2008). Specificity of ADAR-mediated RNA editing in newly identified targets. *RNA (New York, N.Y.)*, *14*(6), 1110–1118. https://doi.org/10.1261/rna.923308

Rodrigues, C. H. M., Pires, D. E. V., & Ascher, D. B. (2021). DynaMut2: Assessing changes in stability and flexibility upon single and multiple point missense mutations. *Protein Science: A Publication of the Protein Society*, *30*(1), 60–69. https://doi.org/10.1002/pro.3942

Rosenthal, J. J. C., & Seeburg, P. H. (2012). A-to-I RNA editing: Effects on proteins key to neural excitability. *Neuron*, *74*(3), 432–439. https://doi.org/10.1016/j.neuron.2012.04.010

Rottner, K., Stradal, T. E. B., & Chen, B. (2021). WAVE regulatory complex. *Current Biology: CB*, *31*(10), Article 10. https://doi.org/10.1016/j.cub.2021.01.086

Saller, E., Tom, E., Brunori, M., Otter, M., Estreicher, A., Mack, D. H., & Iggo, R. (1999). Increased apoptosis induction by 121F mutant p53. *The EMBO Journal*, *18*(16), 4424–4437. https://doi.org/10.1093/emboj/18.16.4424

Sayad, A., Ranjbaran, F., Ghafouri-Fard, S., Arsang-Jang, S., & Taheri, M. (2018). Expression Analysis of CYFIP1 and CAMKK2 Genes in the Blood of Epileptic and Schizophrenic Patients. *Journal of Molecular Neuroscience: MN*, *65*(3), 336–342. https://doi.org/10.1007/s12031-018-1106-2

Schacher, S. (1992). Culturing nerve cells. *Biological Psychology*, *33*(2–3), 266–268. https://doi.org/10.1016/0301-0511(92)90040-2

Schaks, M., Reinke, M., Witke, W., & Rottner, K. (2020). Molecular Dissection of Neurodevelopmental Disorder-Causing Mutations in CYFIP2. *Cells*, *9*(6), 1355. https://doi.org/10.3390/cells9061355

Schaks, M., Singh, S. P., Kage, F., Thomason, P., Klünemann, T., Steffen, A., Blankenfeldt, W., Stradal, T. E., Insall, R. H., & Rottner, K. (2018). Distinct Interaction Sites of Rac GTPase with WAVE Regulatory Complex Have Non-redundant Functions in Vivo. *Current Biology: CB*, *28*(22), 3674-3684.e6. https://doi.org/10.1016/j.cub.2018.10.002

Schenck, A., Bardoni, B., Moro, A., Bagni, C., & Mandel, J. L. (2001). A highly conserved protein family interacting with the fragile X mental retardation protein (FMRP) and displaying selective interactions with FMRP-related proteins FXR1P and FXR2P. *Proceedings of the National Academy of Sciences of the United States of America*, *98*(15), 8844–8849. https://doi.org/10.1073/pnas.151231598

Schindelin, J., Arganda-Carreras, I., Frise, E., Kaynig, V., Longair, M., Pietzsch, T., Preibisch, S., Rueden, C., Saalfeld, S., Schmid, B., Tinevez, J.-Y., White, D. J., Hartenstein, V., Eliceiri, K., Tomancak, P., & Cardona, A. (2012). Fiji: An open-source platform for biological-image analysis. *Nature Methods*, *9*(7), 676–682. https://doi.org/10.1038/nmeth.2019

Shah, K., & Rossie, S. (2018). Tale of the Good and the Bad Cdk5: Remodeling of the Actin Cytoskeleton in the Brain. *Molecular Neurobiology*, *55*(4), Article 4. https://doi.org/10.1007/s12035-017-0525-3

Shimokawa, T., Rahman, M. F.-U., Tostar, U., Sonkoly, E., Ståhle, M., Pivarcsi, A., Palaniswamy, R., & Zaphiropoulos, P. G. (2013). RNA editing of the GLI1 transcription factor modulates the output of Hedgehog signaling. *RNA Biology*, *10*(2), 321–333. https://doi.org/10.4161/rna.23343

Shtrichman, R., Germanguz, I., Mandel, R., Ziskind, A., Nahor, I., Safran, M., Osenberg, S., Sherf, O., Rechavi, G., & Itskovitz-Eldor, J. (2012). Altered A-to-I RNA editing in human embryogenesis. *PloS One*, *7*(7), e41576. https://doi.org/10.1371/journal.pone.0041576

Silva, A. I., Haddon, J. E., Ahmed Syed, Y., Trent, S., Lin, T.-C. E., Patel, Y., Carter, J., Haan, N., Honey, R. C., Humby, T., Assaf, Y., Owen, M. J., Linden, D. E. J., Hall, J., & Wilkinson, L. S. (2019). Cyfip1 haploinsufficient rats show white matter changes, myelin thinning, abnormal oligodendrocytes and behavioural inflexibility. *Nature Communications*, *10*(1), 3455. https://doi.org/10.1038/s41467-019-11119-7

Sommer, B., Köhler, M., Sprengel, R., & Seeburg, P. H. (1991). RNA editing in brain controls a determinant of ion flow in glutamate-gated channels. *Cell*, *67*(1), 11–19. https://doi.org/10.1016/0092-8674(91)90568-j

Su, A. I., Wiltshire, T., Batalov, S., Lapp, H., Ching, K. A., Block, D., Zhang, J., Soden, R., Hayakawa, M., Kreiman, G., Cooke, M. P., Walker, J. R., & Hogenesch, J. B. (2004). A gene atlas of the mouse and human protein-encoding transcriptomes. *Proceedings of the National Academy of Sciences of the United States of America*, *101*(16), 6062–6067. https://doi.org/10.1073/pnas.0400782101

Suraneni, P., Rubinstein, B., Unruh, J. R., Durnin, M., Hanein, D., & Li, R. (2012). The Arp2/3 complex is required for lamellipodia extension and directional fibroblast cell migration. *The Journal of Cell Biology*, *197*(2), 239–251. https://doi.org/10.1083/jcb.201112113

Takenawa, T., & Suetsugu, S. (2007). The WASP-WAVE protein network: Connecting the membrane to the cytoskeleton. *Nature Reviews. Molecular Cell Biology*, *8*(1), 37–48. https://doi.org/10.1038/nrm2069

Tariq, A., & Jantsch, M. F. (2012). Transcript diversification in the nervous system: a to I RNA editing in CNS function and disease development. *Frontiers in neuroscienc*e, 6, 99. https://doi.org/10.3389/fnins.2012.00099

Tiwari, S. S., Mizuno, K., Ghosh, A., Aziz, W., Troakes, C., Daoud, J., Golash, V., Noble, W., Hortobágyi, T., & Giese, K. P. (2016). Alzheimer-related decrease in CYFIP2 links amyloid production to tau hyperphosphorylation and memory loss. *Brain: A Journal of Neurology*, *139*(Pt 10), 2751–2765. https://doi.org/10.1093/brain/aww205

Tran, S. S., Jun, H.-I., Bahn, J. H., Azghadi, A., Ramaswami, G., Van Nostrand, E. L., Nguyen, T. B., Hsiao, Y.-H. E., Lee, C., Pratt, G. A., Martínez-Cerdeño, V., Hagerman, R. J., Yeo, G. W., Geschwind, D. H., & Xiao, X. (2019). Widespread RNA editing dysregulation in brains from autistic individuals. *Nature Neuroscience*, *22*(1), 25–36. https://doi.org/10.1038/s41593-018-0287-x

Wahlstedt, H., Daniel, C., Ensterö, M., & Ohman, M. (2009). Large-scale mRNA sequencing determines global regulation of RNA editing during brain development. *Genome Research*, *19*(6), 978–986. https://doi.org/10.1101/gr.089409.108

Yanai, I., Benjamin, H., Shmoish, M., Chalifa-Caspi, V., Shklar, M., Ophir, R., Bar-Even, A., Horn-Saban, S., Safran, M., Domany, E., Lancet, D., & Shmueli, O. (2005). Genome-wide midrange transcription profiles reveal expression level relationships in human tissue specification. *Bioinformatics (Oxford, England)*, *21*(5), 650–659. https://doi.org/10.1093/bioinformatics/bti042

Zhang, Y., Kang, H., Lee, Y., Kim, Y., Lee, B., Kim, J. Y., Jin, C., Kim, S., Kim, H., & Han, K. (2018). Smaller Body Size, Early Postnatal Lethality, and Cortical Extracellular Matrix-Related Gene Expression Changes of Cyfip2-Null Embryonic Mice. *Frontiers in Molecular Neuroscience*, *11*, 482. https://doi.org/10.3389/fnmol.2018.00482

Zhang, Y., Kang, H. R., & Han, K. (2019). Differential cell-type-expression of CYFIP1 and CYFIP2 in the adult mouse hippocampus. *Animal Cells and Systems*, *23*(6), 380–383. https://doi.org/10.1080/19768354.2019.1696406

Zweier, M., Begemann, A., McWalter, K., Cho, M. T., Abela, L., Banka, S., Behring, B., Berger, A., Brown, C. W., Carneiro, M., Chen, J., Cooper, G. M., Deciphering Developmental Disorders (DDD) Study, Finnila, C. R., Guillen Sacoto, M. J., Henderson, A., Hüffmeier, U., Joset, P., Kerr, B., … Rauch, A. (2019). Spatially clustering de novo variants in CYFIP2, encoding the cytoplasmic FMRP interacting protein 2, cause intellectual disability and seizures. *European Journal of Human Genetics: EJHG*, *27*(5), 747–759. https://doi.org/10.1038/s41431-018-0331-z